Plant Biotechnology Journal
Open Access

Plant Biotechnology Journal (2024) **22**, pp. 1352–1371 doi: 10.1111/pbi.14271

OsGELP77, a QTL for broad-spectrum disease resistance and yield in rice, encodes a GDSL-type lipase

Miaojing Zhang†, Dan Chen†, Jingjing Tian, Jianbo Cao, Kabin Xie, Yuqing He and Meng Yuan*

National Key Laboratory of Crop Genetic Improvement, National Center of Plant Gene Research (Wuhan), Hubei Hongshan Laboratory, Huazhong Agricultural University, Wuhan, China

Received 9 October 2023;
revised 15 November 2023;
accepted 29 November 2023.
*Correspondence (Tel 86-27-87281812; fax 86-27-87287092; email myuan@mail.hzau.edu.cn)
†These authors contributed equally to this work.

Keywords: disease resistance, lipase, *OsGELP77*, OsWRKY45, QTL, rice.

Summary

Lipids and lipid metabolites have essential roles in plant–pathogen interactions. GDSL-type lipases are involved in lipid metabolism modulating lipid homeostasis. Some plant GDSLs modulate lipid metabolism altering hormone signal transduction to regulate host-defence immunity. Here, we functionally characterized a rice lipase, OsGELP77, promoting both immunity and yield. *OsGELP77* expression was induced by pathogen infection and jasmonic acid (JA) treatment. Overexpression of *OsGELP77* enhanced rice resistance to both bacterial and fungal pathogens, while loss-of-function of *osgelp77* showed susceptibility. OsGELP77 localizes to endoplasmic reticulum and is a functional lipase hydrolysing universal lipid substrates. Lipidomics analyses demonstrate that OsGELP77 is crucial for lipid metabolism and lipid-derived JA homeostasis. Genetic analyses confirm that OsGELP77-modulated resistance depends on JA signal transduction. Moreover, population genetic analyses indicate that *OsGELP77* expression level is positively correlated with rice resistance against pathogens. Three haplotypes were classified based on nucleotide polymorphisms in the *OsGELP77* promoter where $OsGELP77^{Hap3}$ is an elite haplotype. Three *OsGELP77* haplotypes are differentially distributed in wild and cultivated rice, while $OsGELP77^{Hap3}$ has been broadly pyramided for hybrid rice development. Furthermore, quantitative trait locus (QTL) mapping and resistance evaluation of the constructed near-isogenic line validated *OsGELP77*, a QTL for broad-spectrum disease resistance. In addition, OsGELP77-modulated lipid metabolism promotes JA accumulation facilitating grain yield. Notably, the hub defence regulator OsWRKY45 acts upstream of OsGELP77 by initiating the JA-dependent signalling to trigger immunity. Together, *OsGELP77*, a QTL contributing to immunity and yield, is a candidate for breeding broad-spectrum resistant and high-yielding rice.

Introduction

GDSL-type lipases/esterases represent a variety of lipolytic enzymes that can hydrolyse diverse lipidic substrates, featured with a conserved GDSL motif GxSxxxG at the N-terminus (Akoh *et al*., 2004; Brick *et al*., 1995). A subgroup GDSLs is further classified as SGNH hydrolase due to four invariant catalytic residues Ser-Gly-Asn-His in the corresponding four conserved blocks. The four catalytic residues are flexible active sites that can change conformation after the binding of different substrates, which contribute to the lipid hydrolase activity and influence the substrate specificity for GDSLs (Akoh *et al*., 2004).

GDSLs are widely distributed in all living species from prokaryotes to eukaryotes. In plants, GDSL gene family consists of a wide range of members, such as 105 members in Arabidopsis (*Arabidopsis thaliana*) and 115 members in rice (*Oryza sativa* L.) (Chepyshko *et al*., 2012; Lai *et al*., 2017; Zhang *et al*., 2020). Accumulating evidence has verified the importance of GDSLs in multiple processes from plant growth and development to biotic and abiotic stress responses (Shen *et al*., 2022). However, only a few plant GDSLs have been referenced with that their substrates are decoded and their broad biological functions are characterized. Some plant GDSLs play important roles in plant immunity through altering lipid metabolism and hormone signalling (Shah, 2005; Shen *et al*., 2022). *Arabidopsis* GDSL LIPASE1 (GLIP1) is a secreted lipase. *GLIP1* regulates pathogen resistance in association with ethylene signalling (Kim *et al*., 2013; Kwon *et al*., 2009). Enhancement of *GLIP1* increased resistance to necrotrophic fungus *Alternaria brassicicola*, necrotrophic bacteria *Erwinia carotovora*, and hemibiotrophic bacteria *Pseudomonas syringae* (Kwon *et al*., 2009), while loss function of *GLIP1* led to susceptible to necrotrophic fungus *Alternaria brassicicola* (Oh *et al*., 2005). *Arabidopsis* GLIP2 possesses lipase activity as GLIP1, however, *GLIP2* and *GLIP1* play distinct roles in response to pathogen attacks that *GLIP2* regulates resistance in association with auxin signalling (Lee *et al*., 2009). *Arabidopsis* AtGDSL1 has lipase activity, playing positive roles in against infection of necrotrophic fungus *Sclerotinia sclerotiorum* (Ding *et al*., 2020). Ectopic expression of *BnGDSL1*, the functional homologue of *AtGDSL1* of *Brassica napus*, in *Nicotiana benthamiana* displayed a significantly reduced disease severity (Ding *et al*., 2020). Rice *OsGLIP1* and *OsGLIP2* are identified as negative regulators of plant immune responses. Simultaneous down-regulation of both of them enhanced rice resistance to bacterial pathogen *Xanthomonas oryzae* pv. *oryzae* (*Xoo*) and fungal pathogen *Magnaporthe oryzae* (*M. oryzae*), while overexpression of these two genes showed compromised defence (Gao *et al*., 2017). However, whether other rice GDSL genes play roles in defence response and even play positive roles in against pathogen attacks are unknown.

GDSLs are lipid-degrading enzymes that have a wide range of substrates due to their flexible conformation (Neves Petersen *et al*., 2001). Several plant GDSLs including Arabidopsis GLIP2, rice OsGLIP1 and OsGLIP2 have lipolytic activity toward universal substrates such as *p*-nitrophenyl acetate or *p*-nitrophenyl butyrate by in vitro lipase activity assays (Gao *et al*., 2017; Lee *et al*., 2009). However, the identification of native substrates for plant GDSLs *in planta* is a great challenge. The biochemical functions of plant GDSLs are largely concluded by in vivo lipidomics analysis that based on which kinds of lipid species have altered contents when GDSL genes are deleted or overexpressed (Gao *et al*., 2017; Lee *et al*., 2009; Shen *et al*., 2022).

Lipid metabolism supplies precursors for jasmonic acid (JA) biosynthesis (Lavell and Benning, 2019). Plastid-targeted rice lipase EG1 participates in JA biosynthesis. The loss-of-function of *eg1* displayed defects in spikelet development and had decreased free JA in spikelets, while exogenous MeJA treatment rescued the abnormal spikelet (Cai *et al*., 2014). As the best-studied lipid metabolite, JA has vital functions as a signal molecule in plant response to pathogen attacks. Rice allene oxide synthase genes *OsAOS1* and *OsAOS2* are two key JA biosynthesis genes in rice. Overexpression of *OsAOS1* and *OsAOS2* in rice increased the endogenous JA level and enhanced rice resistance to *Xoo* and *M. oryzae* (Hou *et al*., 2019; Mei *et al*., 2006). In plants, some minor perturbation in lipid homeostasis has direct consequences on JA signalling (Lavell and Benning, 2019). Both *Arabidopsis* AtPAD4 and rice OsPAD4 are lipases, while they adopt different mechanisms against pathogen infection. *AtPAD4* plays a negative role in response to pathogen infection relying on JA signalling pathway (Brodersen *et al*., 2006), while *OsPAD4* plays a positive role in the fight against pathogen by enhancing JA accumulation (Ke *et al*., 2014). The deciphered mechanisms support that both JA accumulation and JA signal transduction play critical roles in mediating defence responses against different pathogens (Ghorbel *et al*., 2021; Wan and Xin, 2022). Moreover, JA plays vital roles in determining grain yield by regulating spikelet formation and development (Deveshwar *et al*., 2020).

Rice serves as the major food crop, its production is restrained by various diseases, such as fungal blast caused by *M. oryzae*, bacterial blight caused by *Xoo*, and bacterial leaf streak caused by *Xanthomonas oryzae* pv. *oryzicola* (*Xoc*), leading to yield loss up to 30% (Deng *et al*., 2020; Kou *et al*., 2010; Zhao *et al*., 2022). Accumulating evidence validates that the most effective and sustainable strategy to control rice diseases is the genetic improvement, including pyramiding *R* genes and resistance quantitative trait locus (QTL). Compared with *R* gene-mediated pathogen race-specific resistance which can be overcome by pathogens in a short time, rice resistance QTL can confer pathogen species-non-specific resistance, that is, durable and broad-spectrum resistance (Deng *et al*., 2020). Although a large number of QTL have been mapped in different rice accessions, the causal QTL genes have finitely been identified and the underlying mechanisms of them against pathogen attack are seldomly characterized (Deng *et al*., 2020; Kou *et al*., 2010; Zhao *et al*., 2022).

Here, we functionally characterized *OsGELP77*, a QTL contributing to broad-spectrum resistance in rice, encodes a GDSL-type lipase. Both in vitro biochemical assays and in vivo lipidomic profiling assays demonstrated that *OsGELP77* modulates lipid metabolism. Overexpression of *OsGELP77* or pyramiding of a natural elite haplotype of *OsGELP77*, *OsGELP77*^{Hap3} which has a high expression level, could significantly increase lipase activity and JA accumulation, resulting in increased resistance to various pathogens and improved yield. In addition, OsWRKY45 directly binds to the *OsGELP77* promoter and activates *OsGELP77* expression, initiating the JA-dependent signalling pathway to trigger immunity. Therefore, our results suggest that *OsGELP77* could be applied for genetic improvement of rice.

Results

Induction of *OsGELP77* expression against pathogen challenge in rice

OsGELP77 expression was induced upon bacterial pathogen *Xoo* infection from our previous transcriptome data (Hong *et al*., 2015). Here, we detailedly analysed *OsGELP77* transcript level in a time course upon *Xoo* infection along with water inoculation as mock control using RT-qPCR assay. In line with transcriptome data, *Xoo* infection induced *OsGELP77* expression, reaching the peak at 12 h post infection (hpi) (Figure S1a), while mock inoculation could not reprogram its transcription. Simultaneously, we assessed *OsGELP77* expression patterns after bacterial pathogen *Xoc* or fungal pathogen *M. oryzae* infection. Similarly, *OsGELP77* expressions were markedly induced when rice leaves were challenged with *Xoc* or *M. oryzae* but not the corresponding mock control (Figure S1b,c), suggesting *OsGELP77* may act as a pathogenic responsive gene. The expression of many pathogenic responsive genes is usually regulated by defence signal molecules such as salicylic acid (SA) or JA (Yang *et al*., 2013). In order to determine whether *OsGELP77* was regulated by these inducers of defence responses, rice leaves were treated with SA and JA along with water as mock control, and then *OsGELP77* expression patterns were analysed. Results showed that *OsGELP77* expressions were elevated upon JA treatment, while were not altered after SA or mock treatment (Figure S1d). Together, these results demonstrate that *OsGELP77* might have roles in rice immune responses.

OsGELP77 positively regulates rice resistance to various pathogens

Because of the activation of *OsGELP77* after bacterial or fungal pathogens infection, it would be reasonable to expect that *OsGELP77* is involved in plant defence against various pathogens. To analyse *OsGELP77* roles in disease resistance, we generated *OsGELP77* overexpressing transgenic plants (*OsGELP77*-OE) in ZH11 where the maize *ubiquitin* promoter was adopted to drive *OsGELP77* expression. Eight independent *OsGELP77*-OE T_0 plants where *OsGELP77* expression levels were significantly increased were selected for further study (Figure S2). Parallelly, loss-of-function mutants of *OsGELP77* were generated by CRISPR/Cas9-mediated mutagenesis in ZH11 background where two sgRNA matching the first exon of *OsGELP77* were designed for Cas9 cleavage (Figure S3a). Two loss-of-function allelic mutants *osgelp77-1* and *osgelp77-2* which contained 99-bp and 100-bp deletions, respectively, in the *OsGELP77* genomic DNA, were selected for the following study (Figure S3b,c). To remove the potential off-targets mutant, the *osgelp77-1* and *osgelp77-2* mutants were backcrossed with wild type ZH11 and generated Cas9-free mutant and wild type pairs for *OsGELP77* gene for subsequent analysis.

We first evaluated disease responses of the *OsGELP77*-OE plant and *osgelp77* mutant to *Xoo*. All the *OsGELP77*-OE T_0 plants had

shorter lesion lengths after *Xoo* PXO99 inoculation than wild type at the booting stage (Figure S2). Furthermore, we inoculated the representative *OsGELP77*-OE plant and *osgelp77* mutant with a set of *Xoo* strains (PXO71, PXO61, PXO341, PXO347). The *OsGELP77*-OE plants displayed enhanced resistance to different *Xoo* strains, as evidenced by 3.2- to 4.2-cm shorter lesion lengths than wild type (Figure 1a,b). In agreement, *Xoo* growth in the *OsGELP77*-OE leaves was decreased, with about 58-fold lower

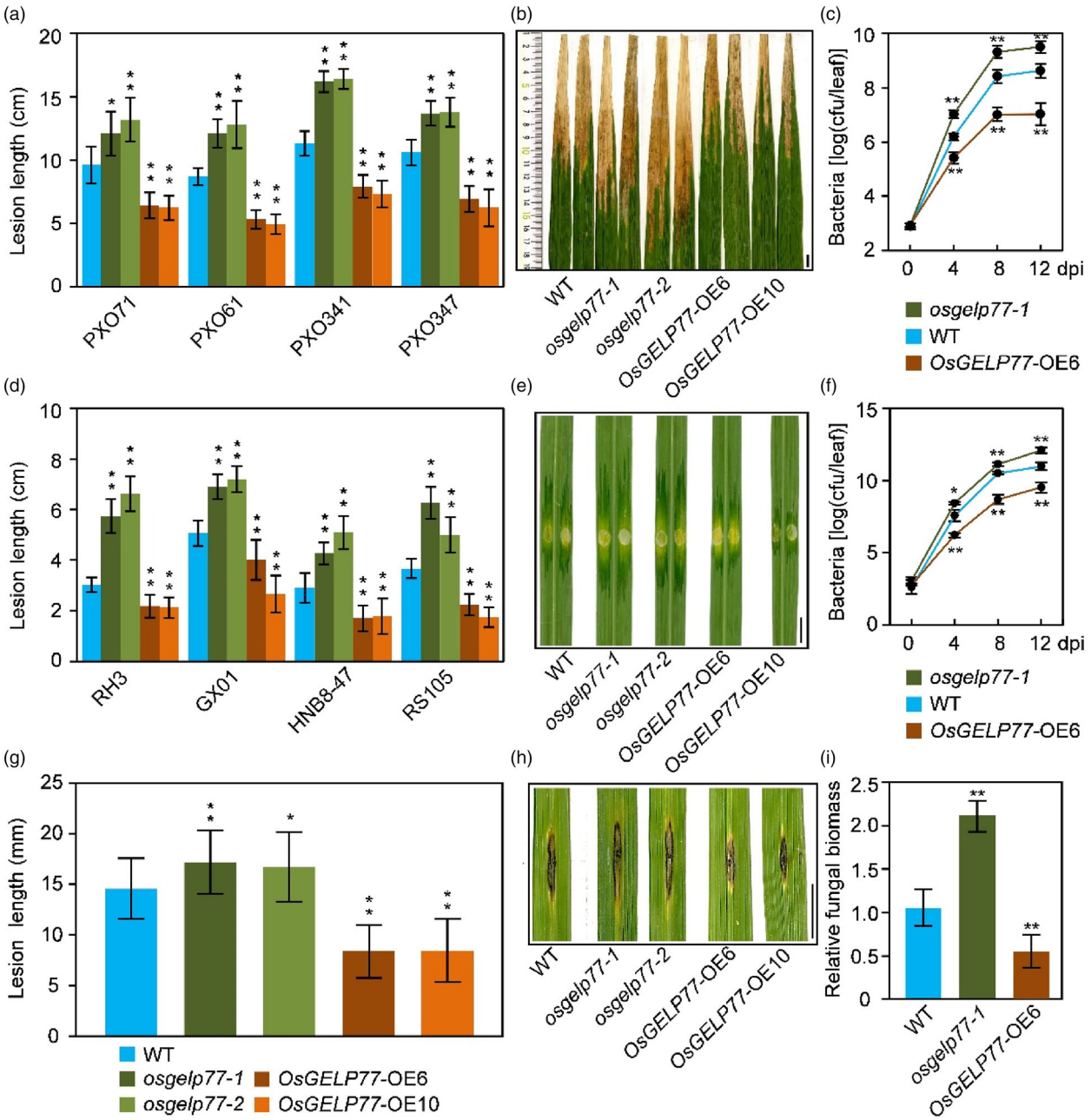

Figure 1 *OsGELP77* positively confers rice resistance to various pathogens. (a) Response of the *OsGELP77*-OE plants and *osgelp77* mutants to different *Xoo* strains. Plants were inoculated with *Xoo* at the booting stage. (b) Phenotype of the *OsGELP77*-OE plants and *osgelp77* mutants after *Xoo* PXO341 infection. Scale bar: 1 cm. (c) Growth of *Xoo* PXO341 in leaves of the *OsGELP77*-OE6 plant and *osgelp77-1* mutant. (d) Response of the *OsGELP77*-OE plants and *osgelp77* mutants to different *Xoc* strains. Plants were inoculated with *Xoc* at the tillering stage. (e) Phenotype of the *OsGELP77*-OE plants and *osgelp77* mutants after *Xoc* RS105 infection. Scale bar: 1 cm. (f) Growth of *Xoc* RS105 in leaves of the *OsGELP77*-OE6 plant and *osgelp77-1* mutant. (g) Response of the *OsGELP77*-OE plants and *osgelp77* mutants to *M. oryzae* isolate 99–20-2. Plants were inoculated with *M. oryzae* at the tillering stage. (h) Phenotype of the *OsGELP77*-OE plants and *osgelp77* mutants after *M. oryzae* infection. Scale bar: 1 cm. (i) Relative fungal biomass of *M. oryzae* in leaves of the *OsGELP77*-OE6 plant and *osgelp77-1* mutant. dpi, days post infection. Data represent means ± SD. $n = 30$ (a, d, g), $n = 6$ (c, f, i). Asterisks in (a, c, d, f, g, i) indicate significant differences between wild type (WT) and the *OsGELP77*-OE plants or *osgelp77* mutants determined by two-tailed Student's *t*-test at $^{**}P < 0.01$ or $^{*}P < 0.05$.

Xoo population at 12 dpi than wild type (Figure 1c). Reversely, the *osgelp77* mutants displayed decreased resistance to these *Xoo* strains, as evidenced by 2.5- to 5.1-cm longer lesion lengths and 26-fold higher *in planta Xoo* population at 12 dpi than wild type (Figure 1a–c).

Then, we investigated *OsGELP77* roles in resistance to *Xoc* by inoculating the *OsGELP77*-OE plant, *osgelp77* mutant, and wild type with different *Xoc* strains (RH3, GX01, HNB8-47, RS105). The *OsGELP77*-OE plants showed enhanced resistance to various *Xoc* strains, with nearly 60%–73% decreased lesion length (Figure 1d,e) and 15- to 40-fold lower *in planta Xoc* population than wild type (Figure 1f). However, the *osgelp77* mutants showed reverse phenotype relative to the *OsGELP77*-OE plants against *Xoc* infection, as evidenced by longer lesion length and more *Xoc* growth than wild type (Figure 1d–f).

In parallel, we punch-inoculated the transgenic plants with *M. oryzae* at the tillering stage using wild type as control. The *OsGELP77*-OE plants showed increased resistance to *M. oryzae* with approximately 41% decreased lesion length, whereas the *osgelp77* mutants showed decreased resistance to *M. oryzae* with about 18% increased lesion length than wild type (Figure 1g,h). Consistently, the *OsGELP77*-OE plants had obviously reduced fungal biomass while the *osgelp77* mutants had increased fungal biomass than wild type (Figure 1i). Taken together, these results indicate that *OsGELP77* positively regulates rice resistance to multiple pathogens.

OsGELP77 has lipase activity

To investigate the spatial expression profile of *OsGELP77*, we examined its expression pattern in different tissues including nodes, sheaths, roots, leaves, and panicles. The RT-qPCR results presented that *OsGELP77* was ubiquitously expressed, with the relatively highest transcription in nodes and the lowest expression in roots (Figure 2a). Moreover, we designed an *OsGELP77pro:GUS* construct where the *OsGELP77* promoter was used to drive the reporter *GUS* gene expression and then transformed the construct into ZH11 to generate transgenic plants. GUS staining of transgenic rice plants expressing *OsGELP77pro:GUS* revealed that the GUS signals were ubiquitously detected in various rice tissues (Figure 2b). The GUS staining results were completely consistent with the RT-qPCR results, confirming the widely expressed pattern of *OsGELP77*.

To analyse the subcellular localization of OsGELP77, we designed a *GFP:OsGELP77* construct where the *OsGELP77* cDNA was downstream fused with the green fluorescent protein (*GFP*) gene and transiently transfected the construct into rice protoplasts. GFP:OsGELP77 exclusively colocalized with HDEL which was upstream fused to the red fluorescent protein (RFP) as an endoplasmic reticulum (ER)-localized marker protein, while GFP:OsGELP77 did not colocalized with chloroplast (Figure 2c), confirming OsGELP77 is an ER protein. Moreover, pathogen-associated molecular pattern flg22 treatment could not alter ER-localized OsGELP77 sublocalization (Figure S4a).

Comparison of OsGELP77 protein sequence with those of functionally characterized paralogues or orthologues showed a high degree of similarity (Figure S4b). Typically, a conserved GDSL motif in the N-terminal and four invariant key catalytic residues (Ser, Gly, Asn, and His) in the functional blocks were invariably presented among these proteins. It hints that OsGELP77 might have lipase activity copying its paralogues or orthologues. To assess the potential lipase activity of OsGELP77, we expressed OsGELP77 in *E. coli* and purified it for activity assay. Because of the signal peptide in the N-terminal, we expressed GST-tagged OsGELP77ΔSP recombinant protein without the signal peptide (Figure 2d). After purification, the recombinant proteins were incubated with four lipid substrates *p*-nitrophenyl butyrate, *p*-nitrophenyl acetate, *p*-nitrophenyl octanoate, and *p*-nitrophenyl palmitate which are generally used for lipase activity assay (Gao *et al.*, 2017). We found OsGELP77ΔSP could hydrolyse these four lipid substrates with high efficiency compared to GST control, and OsGELP77 preferred to hydrolyse *p*-nitrophenyl butyrate in these four substrates (Figure 2e), suggesting that OsGELP77 processes a lipase activity. Simultaneously, we expressed GST-tagged OsGELP77^{4A}ΔSP recombinant protein where the four invariant key catalytic residues in the functional blocks were mutated to alanine. Unsurprisingly, the purified OsGELP77^{4A}ΔSP protein completely could not hydrolyse these four lipid substrates (Figure 2e), demonstrating the key role of the four conserved catalytic residues. In addition, we measured the lipase activity of total proteins in the leaves of *OsGELP77* transgenic plants. Lipase activity of total proteins from the *OsGELP77*-OE plants was higher, while that from the *osgelp77* mutants was lower than wild type (Figure 2f). Together, these results suggest that ER-localized OsGELP77 is a functional lipase.

OsGELP77 modulates lipid metabolism

To uncover the role of OsGELP77 in lipid metabolism, we conducted lipidomic profiling on leaves of the *OsGELP77* transgenic plants. A total of 12 classes of lipids including phosphatidic acid (PA), phosphatidylcholine (PC), phosphatidylethanolamine (PE), phosphatidylglycerol (PG), phosphatidylinositol (PI), phosphatidylserine (PS), free fatty acids (FFA), diacylglycerol (DAG), triacylglycerol (TAG), digalactosyldiacylglycerol (DGDG), monogalactosyldiacylglycerol (MGDG), and sulfoquinovosyldiacylglycerol (SQDG) were identified and quantified by LC-ESI-MS/MS. Total contents of PA, PS, FFA, and TAG were significantly higher in the *OsGELP77*-OE plants, while lower in the *osgelp77* mutants than wild type. Reversely, total levels of PG, PI, and DAG were obviously decreased in the *OsGELP77*-OE plants, while increased in the *osgelp77* mutants than wild type (Figure 3a). Moreover, total contents of PC, PE, DGDG, MGDG, and SQDG had no significant difference between in these transgenic plants and wild type.

We further quantified the contents of 379 individual lipid molecular species in the *OsGELP77*-OE plant and *osgelp77* mutant. Seven of eight PA species were accumulated in the *OsGELP77*-OE plants and decreased in the *osgelp77* mutants than wild type, except for 16:0/18:2 PA which had comparable levels in the transgenic plants and wild type (Figure 3b). Seven PS species all had enhanced accumulation in the *OsGELP77*-OE plants and declined levels in the *osgelp77* mutants relative to wild type (Figure 3c). For PG, we quantified and analysed 31 PG species, eight of them had lower contents in the *OsGELP77*-OE plants, while 13 of them had higher levels in the *osgelp77* mutants than wild type (Figure 3d). For 12 PI species, only two of them (18:1/18:2, 18:2/18:2) had decreased contents in the *OsGELP77*-OE plants, and increased levels in the *osgelp77* mutants than wild type (Figure 3e). The quantified 29 PC and 20 PE species had similar contents between in transgenic plants and wild type (Figure S5a,b). Moreover, we quantified 28 FFA and found that the *OsGELP77*-OE plants had a significant accumulation of 18:1 and 18:2, whereas the *osgelp77* mutants had an obvious decline of 18:1 and 18:2 (Figure S6). We further quantified and analysed 26 DGDG, 37 MGDG, and 25 SQDG in the transgenic plant leaves. Although there were similar total

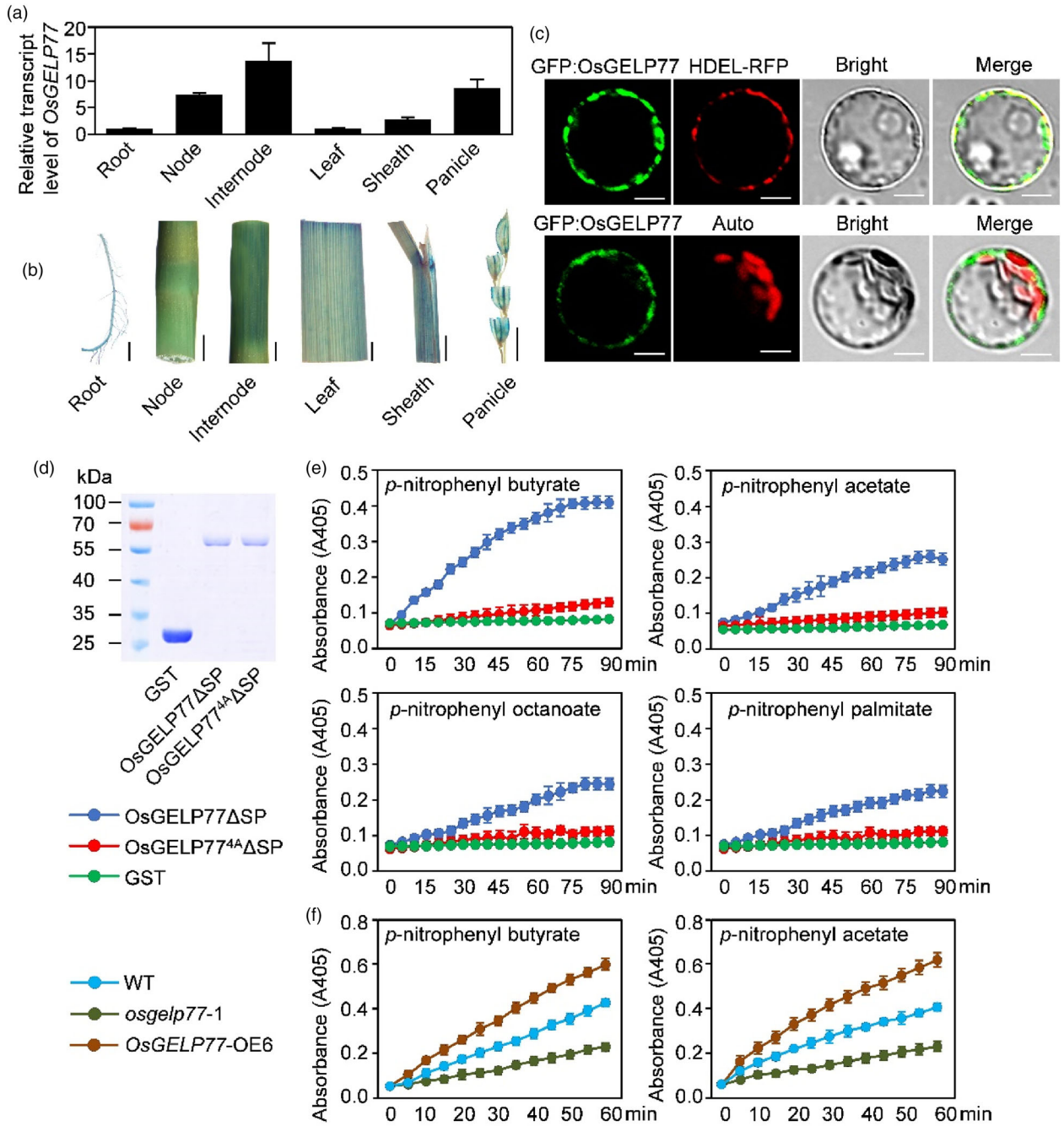

Figure 2 Expression patterns of *OsGELP77* and lipase activity of OsGELP77. (a) *OsGELP77* expression in different tissues. Data represent means ± SD (n = 3). Gene expression analysis was performed by RT-qPCR and normalized to *Actin*. (b) Histochemical staining of different tissues of *OsGELP77pro:Gus* transgenic lines. Scale bars: 1 cm. (c) Subcellular localization of OsGLEP77 in rice protoplasts. HDEL protein fused to RFP was used as an endoplasmic reticulum marker. Auto, chlorophyll autofluorescence. Scale bars: 10 μm. (d) Expression and purification of recombinant OsGELP77ΔSP-GST and OsGELP77^{4A}ΔSP-GST proteins in *E. coli*. (e) Recombinant OsGELP77ΔSP-GST and OsGELP77^{4A}ΔSP-GST proteins were incubated with *p*-nitrophenyl butyrate, *p*-nitrophenyl acetate, *p*-nitrophenyl octanoate, or *p*-nitrophenyl palmitate. The absorbance readings were collected every 5 min in a time course of 90 min. (f) Total proteins from the leaves of transgenic plants and wild type (WT) were incubated with *p*-nitrophenyl butyrate and *p*-nitrophenyl acetate. The absorbance readings were collected every 5 min in a time course of 60 min. Data represent means ± SD. n = 6 (e, f).

contents of DGDG, MGDG, or SQDG between in the *OsGELP77*-OE plants or the *osgelp77* mutants and wild type, five DGDG species (Figure S7), six MGDG species (Figure S8), and four SQDG species (Figure S9) had altered contents. In addition, we analysed 49 DAG and 107 TAG contents, with the results that at least three DAG had lower levels in the *OsGELP77*-OE plants and higher levels in the *osgelp77* mutants (Figure S10), whereas one-third of TAG species had enhanced contents in the *OsGELP77*-OE plants and decreased contents in the *osgelp77* mutants (Figure S11), relative to those in wild type.

To further analyse the lipidomic data, we performed KEGG enrichment analysis to annotate the potential implication of

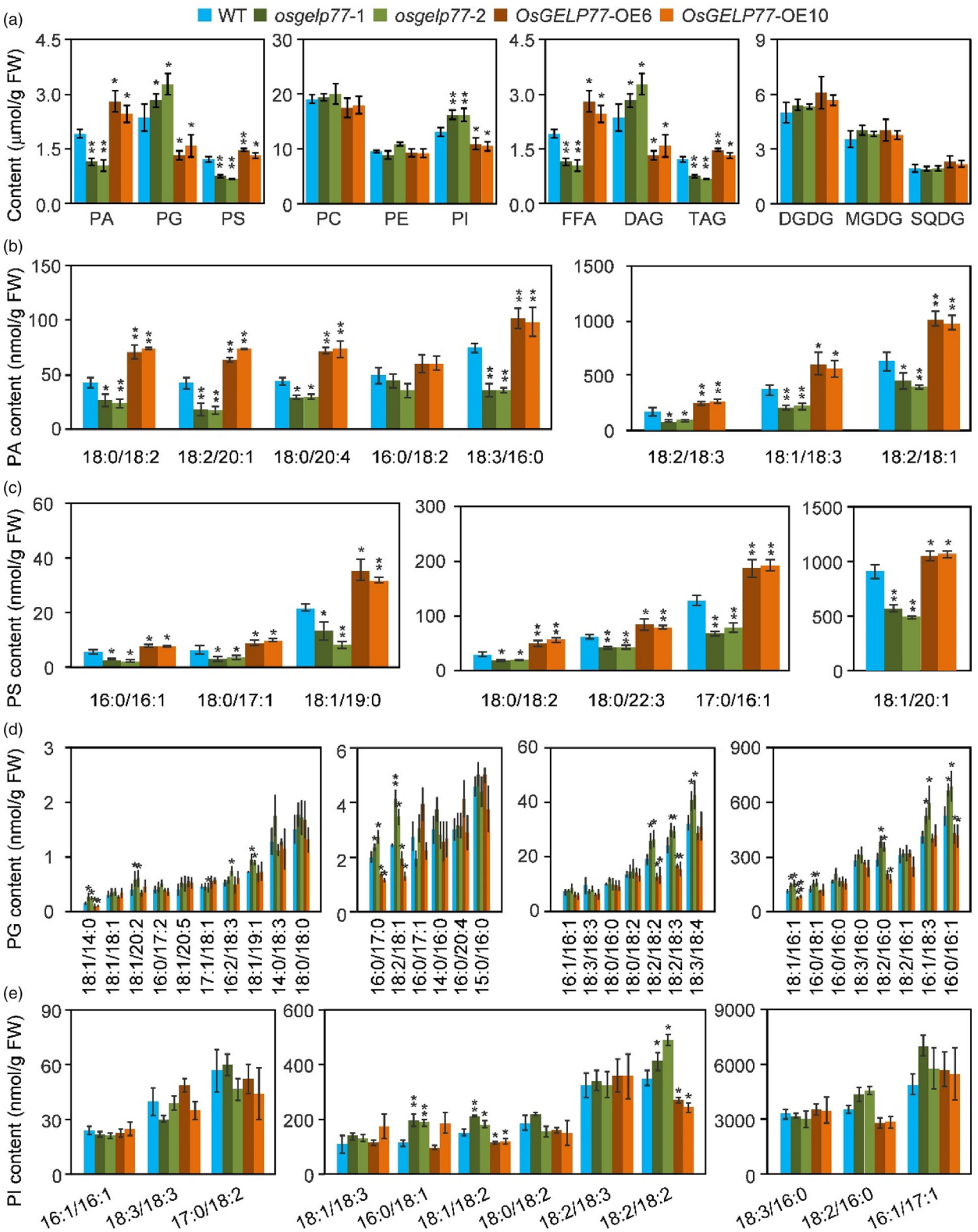

Figure 3 Lipidomic profiling of the *OsGELP77*-OE plants and *osgelp77* mutants. (a) Total lipid composition in the leaves of transgenic plants and wild type (WT). (b) Contents of eight PA species. (c) Contents of seven PS species. (d) Contents of 31 PG species. (e) Contents of 12 PI species. The individual lipid species is presented as the XX:Y nomenclature where XX is the number of carbon atoms and Y is the number of double bonds in the fatty acyl groups. Data represent means ± SD (n = 3). Asterisks in (a–e) indicate significant differences between WT and the *OsGELP77*-OE plants or *osgelp77* mutants determined by two-tailed Student's t-test at $^{**}P < 0.01$ or $^{*}P < 0.05$.

different lipids. The major enriched metabolic pathways both in the *OsGELP77*-OE plant and the *osgelp77* mutant were glycerolipid metabolism, glycerophospholipid metabolism, and sphingolipid metabolism (Figure S12a,b), suggesting that the altered metabolic pathways were associated with the biochemical function of OsGELP77.

OsGELP77-modulated lipid metabolism alters JA homeostasis

To decipher the underlying mechanism of OsGELP77-modulated lipid metabolism participating in immune response, we analysed the transcriptome profile of the *osgelp77* mutant and wild type leaves. Totally, 106 up-regulated differentially expressed genes (DEGs) and 100 down-regulated DEGs were identified in the *osgelp77* mutant compared with wild type (Tables S1 and S2). The GO term analysis showed that enriched GO terms for biological process included JA-mediated signalling pathway. KEGG pathway enrichment analysis presented that the mainly enriched pathway contained plant hormone signal transduction. Both the GO and KEGG enrichment analysis for DEGs of *OsGELP77* were related with JA (Figure S13), which echoed with the infer that OsGELP77 modulates lipid metabolism as JA is lipid-derived phytohormone.

Among the DEGs, *OsJAZ8*, acting as a repressor of JA signalling and negatively regulating the JA-induced resistance to *Xoo* (Sun *et al*., 2022; Yamada *et al*., 2012), had enhanced level in the *osgelp77* mutant, while *OsMYC2* encoding a global regulator of JA signalling and positively regulating rice resistance against *Xoo* (Uji *et al*., 2016), had compromised expression in the *osgelp77* mutant. RT-qPCR assays confirmed higher expression of *OsJAZ8* and lower expression of *OsMYC2* in the *osgelp77* mutant, and reversely, lower expression of *OsJAZ8* and higher expression of *OsMYC2* in the *OsGELP77*-OE plant (Figure S14). Since *OsJAZ8* and *OsMYC2* are induced by JA and pathogens, participating in JA-dependent signal transduction (Uji *et al*., 2016; Yamada *et al*., 2012). The expressions of *OsJAZ8* and *OsMYC2* were induced in the leaves of *OsGELP77*-OE plants, *osgelp77* mutants, and wild type after *Xoo* inoculation, however, the induced tendency was obviously higher for *OsMYC2* in the *OsGELP77*-OE plant and *OsJAZ8* in the *osgelp77* mutant than those in wild type (Figure S14).

The above results promoted us to evaluate JA content in the transgenic plants. Consistent with altered lipid homeostasis and changed expression patterns of JA-dependent signalling pathway genes, JA contents were 2.1- to 2.3-fold higher in the *OsGELP77*-OE plants and 1.9- to 2.7-fold lower in the *osgelp77* mutants than wild type (Figure 4a). In agreement, expression levels of *OsLOX2* and *OsAOS2*, which two are JA biosynthesis genes (Ghorbel *et al*., 2021), were significantly higher in the *OsGELP77*-OE plants and lower in the *osgelp77* mutants relative to wild type (Figure 4b). Accordingly, JA-responsive pathogen-related *PR* genes such as *OsPR1a*, *OsPR1b*, and *OsPR5* had significantly enhanced expression levels in the *OsGELP77*-OE plants and attenuated expressions in the *osgelp77* mutants than wild type (Figure 4c). Moreover, SA content and transcript levels of two representative SA-responsive genes were comparable between in the *OsGELP77*-OE plants or *osgelp77* mutants and wild type (Figure 4d,e). These results further support that OsGELP77-modulated lipid metabolism alters JA content.

Since JA inhibits seedling growth in plants and this property has been widely used in JA synthesis- and signalling-related mutant selection (Deng *et al*., 2012). A seed germination assay was carried out to analyse the effects of methyl jasmonate (MeJA) on the growth of *OsGELP77* transgenic plants. The results showed that root and shoot elongation of the *OsGELP77*-OE plants were more sensitive to MeJA treatment, while root and shoot elongation of the *osgelp77* mutants were less sensitive to MeJA application relative to wild type (Figure S15a,b). Taken together, these results suggest that OsGELP77-modulated lipid metabolism positively regulates JA homeostasis.

OsGELP77-modulated resistance depends on JA signalling

Since both enhanced JA levels and activated JA signalling mediate plant resistance to pathogen infections (Campos *et al*., 2014; Zhang *et al*., 2017b). To further confirm whether *OsGELP77*-mediated resistance depends on JA levels or JA signalling, we crossed the *OsGELP77*-OE plant with *coi1-13* which is a JA-insensitive rice line in Nipponbare (Nip) background. In *coi1-13*, JA signalling receptor genes *OsCOI1A* and *OsCOI1B* were knocked down and JA signal transduction was disrupted (Yang *et al*., 2012). We found overexpression of *OsGELP77* could significantly accumulate JA in *coi1-13* as that in Nip (Figure 5a). In agreement, overexpression of *OsGELP77* could activate the transcription of JA-responsive gene *OsVSP* which functions downstream of *OsCOI1* in JA signal transduction (Yang *et al*., 2012), in Nip. However, overexpression of *OsGELP77* could not induce *OsVSP* expression in *coi1-13* although there was abundance of JA content (Figure 5b). Accordingly, overexpression of *OsGELP77* increased rice resistance to *Xoo* in Nip, while could not enhance resistance in *coi1-13* (Figure 5c), suggesting that *OsGELP77*-mediated resistance largely depends on JA signal transduction.

Parallelly, we overexpressed *OsGELP77* in the *osmyc2* mutant (Qiu *et al*., 2022), to evaluate the relationship between JA signalling disruption and *OsGELP77*-mediated resistance (Figure S16). Overexpression of *OsGELP77* in *osmyc2* mutant could also enhance JA accumulation (Figure 5d). However, *OsGELP77* overexpressing could not heighten *OsVSP* expression in *osmyc2* (Figure 5e), and could not reverse the susceptibility of *osmyc2* mutant to *Xoo* (Figure 5f). These data together suggest that JA signalling disruption can attenuate *OsGELP77*-mediated rice resistance.

In addition, to experimentally confirm whether *OsGELP77*-mediated resistance was JA signalling dependent, we analysed the response of the *OsGELP77*-OE plant or *osgelp77* mutant to exogenous application of JA. Previous study has validated that exogenous JA treatment reduces the susceptibility of rice to *Xoo* (Ke *et al*., 2014). Consistent with previous results, exogenous JA treatment enhanced rice resistance to *Xoo* in the *osgelp77* mutant and wild type, as evidenced by the shorter lesion length compared with mock-treated plants (Figure 5g). JA application could complement the susceptibility of the *osgelp77* mutant, that the mutant even showed shorter lesion length than mock-treated wild type. Knockout of *OsGELP77* compromised the enhanced resistance to *Xoo* conferred by exogenous JA application, however, the *osgelp77* mutant had fewer reduced lesion length compared with JA-treated wild type. A similar pattern was observed that exogenous JA treatment could clearly enhance resistance to *Xoc* in the *osgelp77* mutant (Figure 5h). Due to high abundance of JA, the enhanced resistance to *Xoo* and *Xoc* was not obviously calculated in the *OsGELP77*-OE plant after exogenous application of JA. Collectively, these results support the inference that OsGELP77-modulated lipid metabolism increases JA content which subsequently heightens JA signal transduction triggering plant immunity.

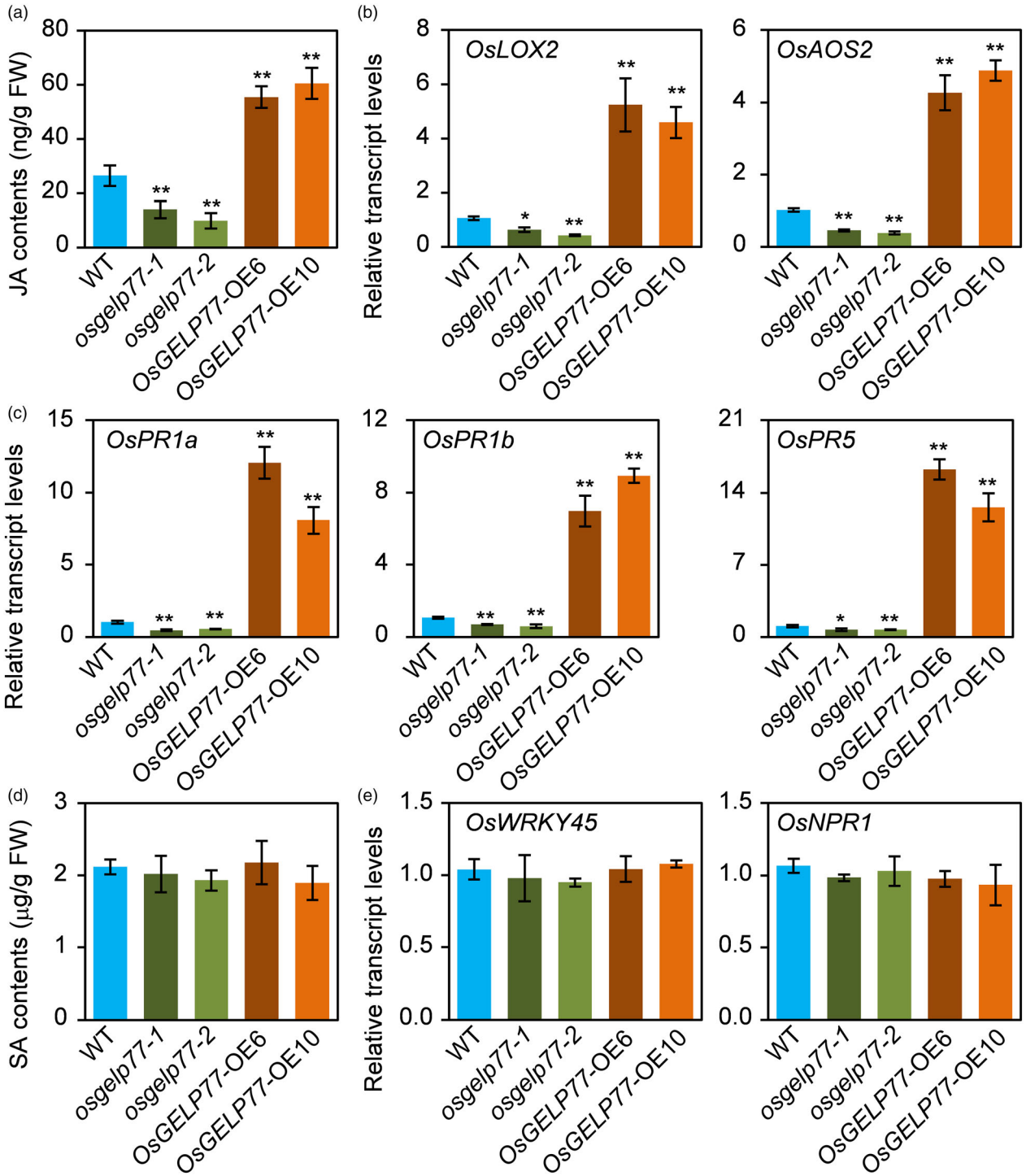

Figure 4 *OsGELP77* Alters JA homeostasis. (a) JA contents in the leaves of transgenic plants and wild type (WT). (b) Relative transcript levels of *OsLOX2* and *OsAOS2* in the leaves of transgenic plants and WT. (c) Relative transcript levels of JA-responsive *PR* genes in the leaves of transgenic plants and WT. (d) SA contents in the leaves of transgenic plants and WT. (e) Relative transcript levels of *OsWRKY45* and *OsNPR1* in the leaves of transgenic plants and WT. Data represent means ± SD ($n = 3$). Gene expression analysis was performed by RT-qPCR and normalized to *Actin*. Asterisks in (a–c) indicate significant differences between WT and the *OsGELP77*-OE plants or *osgelp77* mutants determined by two-tailed Student's *t*-test at $^{**}P < 0.01$ or $^{*}P < 0.05$.

OsGELP77-modulated lipid metabolism modifies agronomic traits

To further investigate the effect of *OsGELP77*-modulated lipid metabolism on rice growth and development, we planted the *OsGELP77*-OE plants and *osgelp77* mutants in the paddy field along with wild type and examined a set of agronomic traits of them. The *OsGELP77*-OE plants had similar agronomic traits including plant height, flag leaf length and width, tiller number, productive panicles per plant, grain width as wild type, while

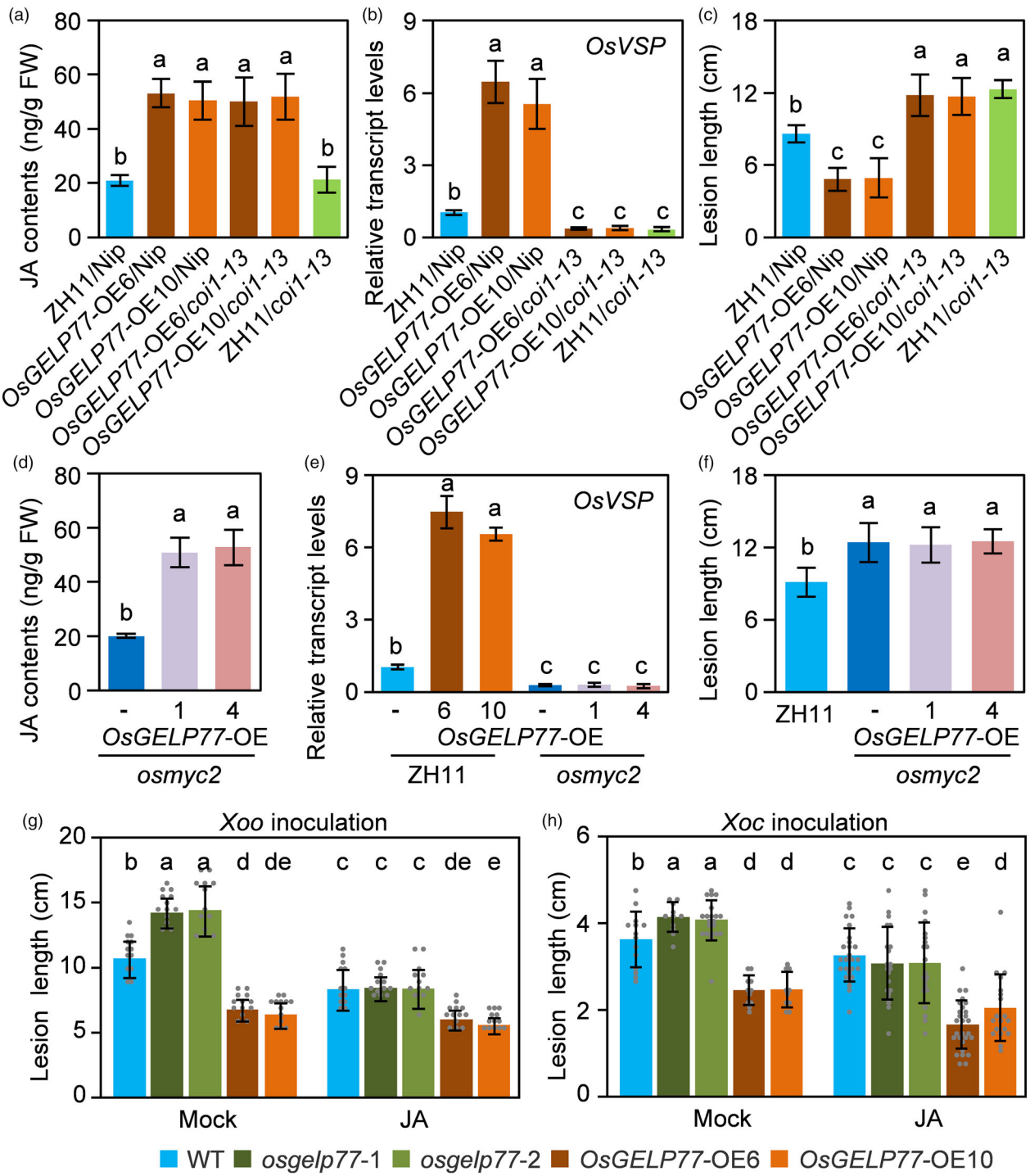

Figure 5 *OsGELP77*-mediated resistance is JA signalling dependent. (a) JA contents in the leaves of transgenic plants and the corresponding background. (b) Relative transcript level of *OsVSP* in the leaves of transgenic plants and the corresponding background. (c) Responses of the transgenic plants and the corresponding background to *Xoo* strain PXO99. (d) JA contents in the leaves of transgenic plants. (e) Relative transcript level of *OsVSP* in the leaves of transgenic plants. (f) Responses of the transgenic plants to *Xoo* strain PXO99. (g) Response of the transgenic plants and wild type (WT) to *Xoo* strain PXO99. (h) Response of the transgenic plants and WT to *Xoc* strain GX01. Plants were pretreated with 250 mM JA and two days later were inoculated with *Xoo* or *Xoc*. Water inoculation was used as mock control. Data represent means ± SD. $n = 3$ (a, b, d, e). $n = 30$ (c, f, g, h). The different letters above each bar in (a, b, c, d, e, f, g, h) indicate statistically significant differences, as determined by one-way ANOVA analysis followed by Tukey's multiple test ($P < 0.05$).

increased panicle length (+4.0% ~ 4.4%), grain length (+2.7% ~ 2.9%), seed setting rate (+4.5% ~ 4.7%), 1000-grain weight (+2.4% ~ 2.8%), and yield per plant (+3.5% ~ 4.8%). Reversely, the *osgelp77* mutants showed decreased tiller number (−19.7% ~ 26.8%), panicle length (−6.1% ~ 9.9%), productive panicles per plant (−14.2% ~ 22.1%), grain length (−1.4% ~ 2.8%),

seed setting rate (−9.5% ~ 13.3%), 1000-grain weight (−2.4% ~ 3.9%), and yield per plant (−7.1% ~ 8.1%) compared with wild type (Figure S17), suggesting that *OsGELP77* has positive effects on agronomic traits.

Natural variation in *OsGELP77*

Given positive roles of *OsGELP77* in disease resistance and agronomic traits, we then investigated its variation in rice germplasm. We compared the sequences of *OsGELP77* in 2178 rice accessions from the RiceVarMap database (http://ricevarmap.ncpgr.cn/), including 80 *tropical japonica*, 481 *temperate japonica*, 823 *indica*, 686 intermediate varieties, and 108 *Aus* rice. Polymorphisms were detected exclusively in the 2-kb promoter but not in the 1942-bp open reading frame, including 6 single-nucleotide polymorphisms (SNPs) distributed in the *OsGELP77* promoter. Therefore, three distinct haplotypes were classified on the basis of nucleotide polymorphisms in the *OsGELP77* promoter (Figure 6a). Of which, *OsGELP77*^{Hap1} and *OsGELP77*^{Hap2} were almost absent in both *tropical japonica* and *temperate japonica*, and *OsGELP77*^{Hap1} was absent in *Aus* rice. An analysis of the geographical distribution of these rice accessions showed that *OsGELP77*^{Hap1} and *OsGELP77*^{Hap2} were mainly distributed in accessions from Asia including China, India, Philippines, Indonesia, and Bangladesh, whereas *OsGELP77*^{Hap3} was distributed in accessions from almost all rice-producing countries/regions (Figure 6b). We then randomly evaluated disease responses of 109 mini-core rice accessions which consist of *tropical japonica*, *temperate japonica*, *indica*, intermediate varieties, and *Aus* rice representing a broad range of rice germplasm (Xie *et al*., 2015). After *Xoo* infection, accessions harbouring *OsGELP77*^{Hap3} had shorter lesion lengths than those containing *OsGELP77*^{Hap1} or *OsGELP77*^{Hap2} (Figure 6c). Accordingly, significantly higher expressions of *OsGELP77* were observed in leaves of accessions harbouring *OsGELP77*^{Hap3} relative to those accessions containing *OsGELP77*^{Hap1} or *OsGELP77*^{Hap2} (Figure 6d). *OsGELP77* expression is positively correlated with the resistance to *Xoo*, supporting its involvement in the regulation of resistance to *Xoo* infection.

Domestication selection of *OsGELP77*

Based on association analysis, two functional SNPs for *OsGELP77* that SNP (T/C) at −1909 bp and SNP (C/T) at −1046 bp were significantly associated with resistance to *Xoo* (Figure 6a). To track the evolution origin of two functional SNPs, we compared *OsGELP77* sequences from 446 geographically diverse accessions of wild rice species *Oryza rufipogon* (Huang *et al*., 2012). The majority of wild rice contains *OsGELP77*^{Hap3} (Figure 6e).

To investigate whether artificial selection has contribution to the domestication of *OsGELP77*, the genomic sequences of 3 k rice accessions were used to analyse the genetic diversity of this gene and its flanking regions. The genetic diversity (π) for *OsGELP77* was relatively lower than its flanking regions (Figure 6f), suggesting a selective sweep at this locus. Among the 12 subgroups of 3 k rice accessions, negative Tajima's *D* values were observed mainly in the *japonica* subpopulation and *indica* subpopulation from South Asia and Southeast Asia but not in the Aus rice and *indica* subpopulation from East Asia (Figure 6g), implying *OsGELP77* underwent differential selection during *japonica* and South or Southeast Asia *indica* rice adaptation.

In addition, we investigated the distribution of different *OsGELP77* haplotypes in 1495 hybrid rice varieties F_1 (Huang *et al*., 2015). Of the 1439 varieties from *indica-indica* hybrid, 20 varieties contain *OsGELP77*^{Hap1} and 543 varieties harbour *OsGELP77*^{Hap3}, while the majority (876 varieties) have *OsGELP77*^{Hap1} and *OsGELP77*^{Hap3}. The 18 varieties from *indica-japonica* hybrid and 38 varieties from *japonica-japonica* hybrid all contain *OsGELP77*^{Hap3} (Figure 6h). The results indicate that the elite allele *OsGELP77*^{Hap3} has been broadly pyramided to develop hybrid rice contributing to rice breeding.

OsGELP77 colocalizes with disease-resistance QTL

Rice accessions containing *OsGELP77*^{Hap3} had high *OsGELP77* expression and showed resistance to *Xoo* compared with those harbouring *OsGELP77*^{Hap1} or *OsGELP77*^{Hap2}, which promoted us a tip that whether *OsGELP77* is a QTL for disease resistance. To support the hypothesis, we retrieved data on disease-related QTL from PubMed, Q-TARO, and RiceQTLPro (Kim *et al*., 2014; Yonemaru *et al*., 2010). We found that *OsGELP77* loci colocalized with previously reported disease-related QTL which were derived using different genetic populations (Figure S18). Rice var Minghui 63 shows moderate resistance to *M. oryzae* isolate V86013 and *Xoo* strain PXO61, rice var Zhenshan 97 is susceptible to these pathogens. Several QTL for disease resistance against *M. oryzae* or *Xoo* were identified in Minghui 63/Zhenshan 97 population (Chen *et al*., 2003; Kou *et al*., 2010). Minghui 63 carries *OsGELP77*^{Hap3} and Zhenshan 97 carries *OsGELP77*^{Hap1}. Moreover, *OsGELP77* expression level was obviously higher in different tissues of Minghui 63 than in Zhenshan 97 (Figure S19). To support that *OsGELP77* is a QTL conferring disease resistance, we mapped *OsGELP77* in a recombinant inbred line (RIL) segregation population developed from a cross between Minghui 63 and Zhenshan 97. The mapping showed that *OsGELP77* colocalized with the curve peak of a resistance QTL against *Xoo* strain PXO61 and a resistance QTL against *M. oryzae* isolate V86013 which explained 6.7% and 6.1% of the phenotypic variation of resistance to PXO61 and V86013 in the population, respectively (Figure 7a). The present results suggest that *OsGELP77* allele from Minghui 63 is most likely a candidate for the gene underlying the resistance QTL.

To experimentally validate *OsGELP77* is a disease-resistance QTL, we constructed the near-isogenic line (NIL) NIL-*OsGELP77*^{Hap3} in the Zhenshan 97 background. Higher *OsGELP77* expression was observed in the NIL-*OsGELP77*^{Hap3} than in Zhenshan 97 (Figure 7b). Accordingly, changes of lipid species levels were observed in the leaves between NIL-*OsGELP77*^{Hap3} and Zhenshan 97. NIL-*OsGELP77*^{Hap3} had higher PA and PS contents and lower PG and PI contents than Zhenshan 97 (Figure 7c). NIL-*OsGELP77*^{Hap3} also had 1.5-fold higher JA accumulation than Zhenshan 97 (Figure 7d). Furthermore, the responses of NIL-*OsGELP77*^{Hap3} and Zhenshan 97 to different pathogens were evaluated. After inoculation with both bacterial pathogens *Xoo* and *Xoc* and fungal pathogen *M. oryzae*, the NIL-*OsGELP77*^{Hap3} exhibited shorter lesion length than its background Zhenshan 97 (Figure 7e–g). These results together support that *OsGELP77* is a QTL contributing to broad-spectrum disease resistance.

Given that *OsGELP77* has been reported acting as a *trans*-eQTL hot spot controlling seed-related agronomic traits (Wang *et al*., 2010). We here confirmed that pyramiding of *OsGELP77*^{Hap3} could enhance seed-related phenotypes, including increased panicle length, 1000-grain weight, and yield per plant

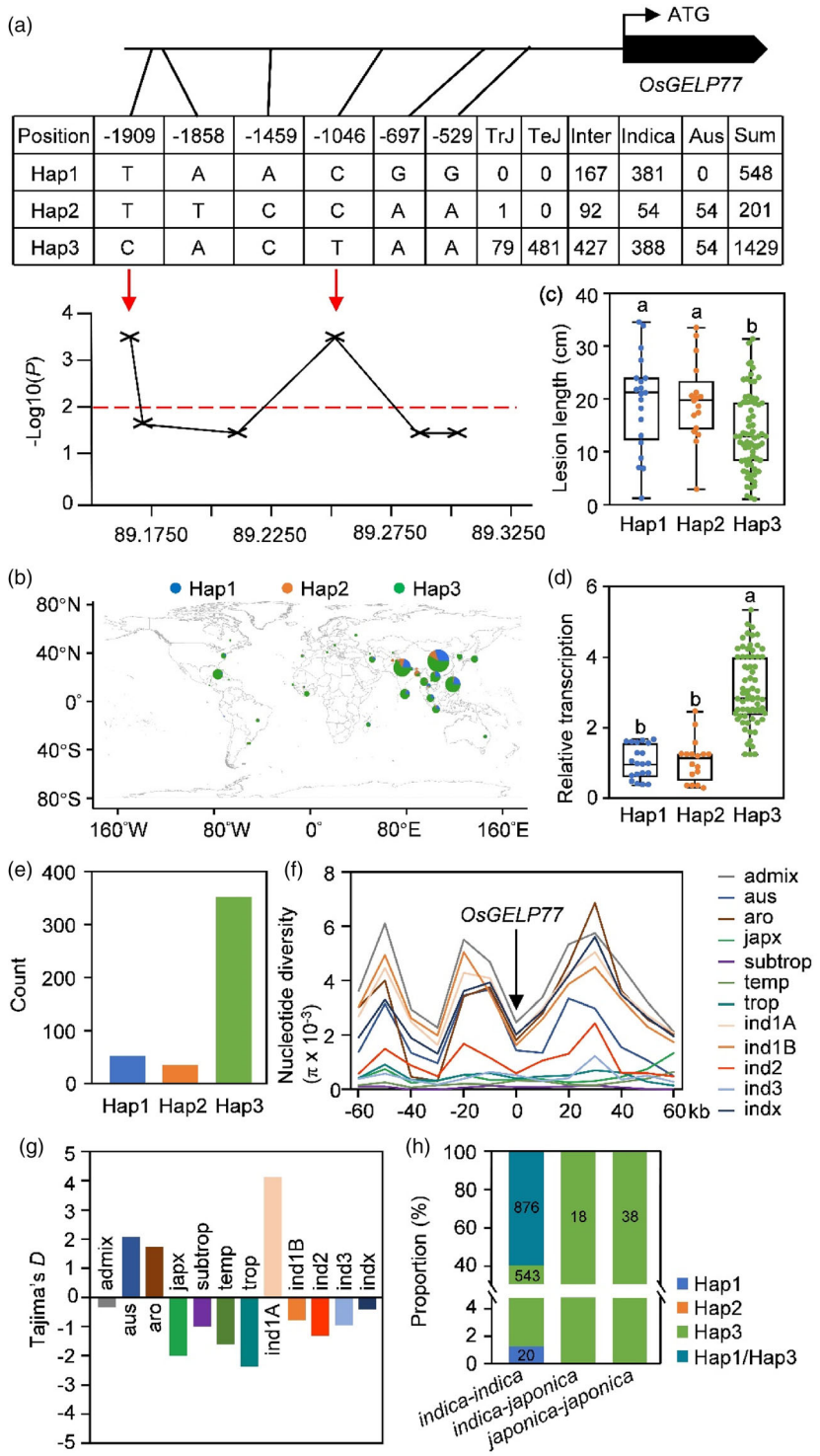

Figure 6 Natural variation in *OsGELP77*. (a) Natural variation and haplotype analysis of *OsGELP77* in 2178 rice accessions. The three haplotypes were based on the six SNPs distributed in the promoter. (b) Geographic distributions of 2178 rice accessions. (c) Disease responses of 109 mini-core rice accessions harbouring three classes of *OsGELP77* haplotype after *Xoo* PXO99 infection. Plants were inoculated with *Xoo* at the booting stage. Data represent means ± SD (n = 30). (d) Relative *OsGELP77* transcript level of the three classes of haplotypes in leaves. Data represent means ± SD (n = 3). (e) Distributions of three *OsGELP77* haplotypes in wild rice. (f) Nucleotide diversity of *OsGELP77* and its surrounding 120-kb region in different rice subgroups. (g) Tajima's *D* values of *OsGELP77* genomic sequences in the subgroups of cultivated rice. (h) Distributions of three *OsGELP77* haplotypes in hybrid rice varieties. The different letters above each bar in (c, d) indicate statistically significant differences, as determined by one-way ANOVA analysis followed by Tukey's multiple test ($P < 0.05$).

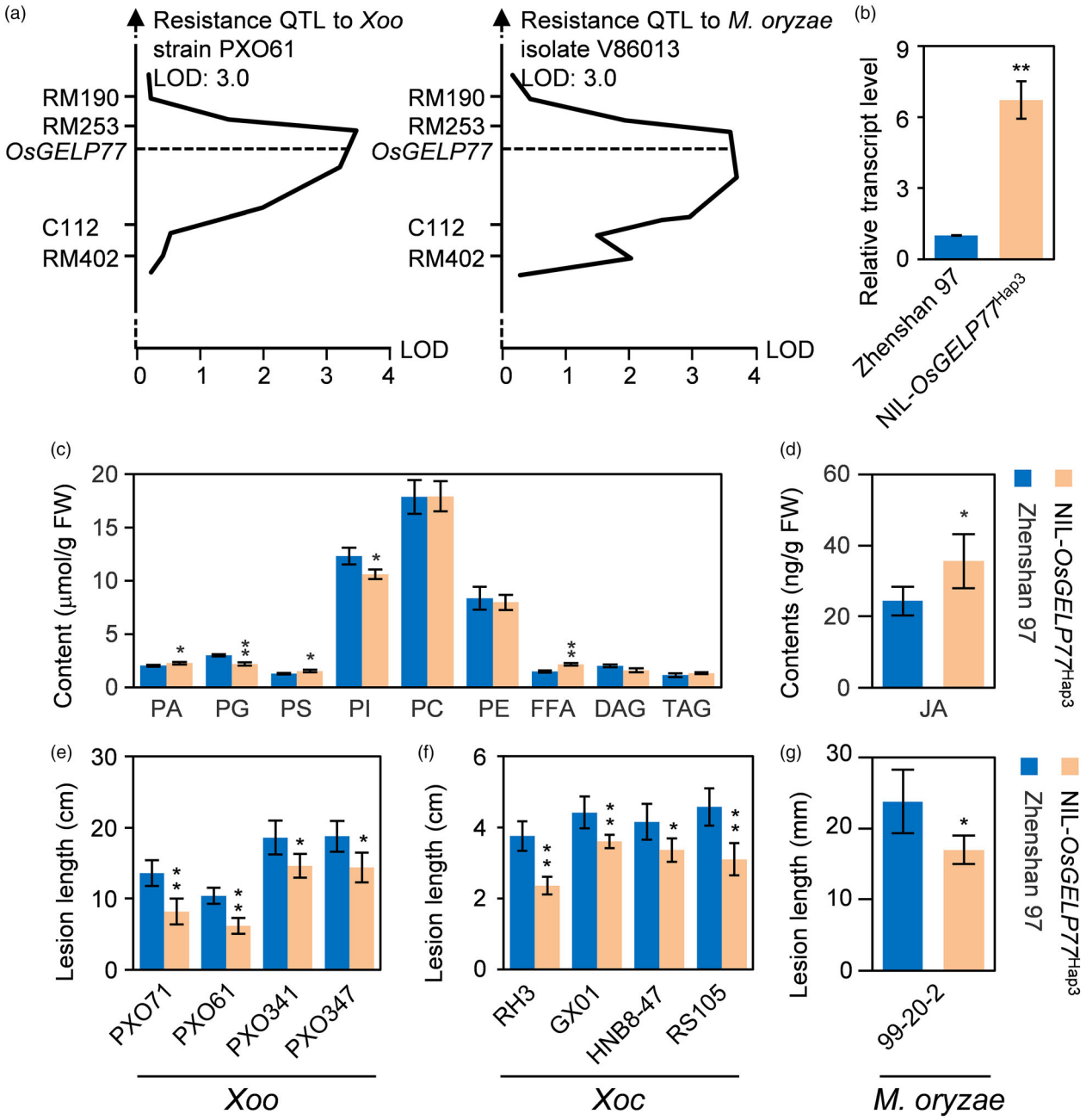

Figure 7 *OsGELP77* is a disease-resistance QTL. (a) Colocalization of *OsGELP77* and disease resistance QTL. LOD, Logarithm of odds. (b) Relative transcript level of *OsGELP77*. (c) Contents of lipid species in the leaves of NIL-*OsGELP77*^{Hap3} and Zhenshan 97. (d) JA content in the leaves of NIL-*OsGELP77*^{Hap3} and Zhenshan 97. (e) Response of NIL-*OsGELP77*^{Hap3} and Zhenshan 97 to different *Xoo* strains. Plants were inoculated with *Xoo* at the booting stage. (f) Response of NIL-*OsGELP77*^{Hap3} and Zhenshan 97 to different *Xoc* strains. Plants were inoculated with *Xoc* at the tillering stage. (g) Response of NIL-*OsGELP77*^{Hap3} and Zhenshan 97 to *M. oryzae* isolate 99–20-2. Plants were inoculated with *M. oryzae* at the tillering stage. Data represent means ± SD. $n = 3$ (b, c, d), $n = 30$ (e, f, g). Asterisks in (b, c, d, e, f, g) indicate significant differences between Zhenshan 97 and NIL-*OsGELP77*^{Hap3} determined by two-tailed Student's *t*-test at $^{**}P < 0.01$ or $^{*}P < 0.05$.

(Figure S20). Collectively, these data indicate that *OsGELP77*^{Hap3} could improve rice immunity and yield.

OsWRKY45 activates *OsGELP77* transcription

In previous studies, *OsWRKY45* has been reported acting as a positive regulator in rice resistance against *Xoo*, *Xoc*, and *M. oryzae*, which was accompanied by increased JA accumulation (Shimono *et al.*, 2012; Tao *et al.*, 2009). The similar mechanism of JA-dependent immunity between *OsWRKY45* and *OsGELP77* encouraged us to test whether OsWRKY45 genetically acts upstream of *OsGELP77*. OsWRKY45 functions as a transcriptional activator binding to the canonical W-box motif with TTGACC core sequence of its downstream target genes (Tao *et al.*, 2009). Notably, the 2-kb *OsGELP77* promoter contains three W-box motifs which might be OsWRKY45 binding sites. To validate that *OsGELP77* is the downstream target gene of OsWRKY45, we conducted a suite of

assays. Firstly, we detected *OsGELP77* transcription in leaf of *OsWRKY45* transgenic plants. RT-qPCR results showed that *OsGELP77* had significantly increased expression in the *OsWRKY45*-OE plants, while decreased expression in the *oswrky45* mutant than in wild type (Figure 8a). Then, to investigate the direct interaction between OsWRKY45 and *OsGELP77* promoter, we conducted EMSA assays to test the binding of OsWRKY45 to the W-box motif in vitro. The prokaryote-expressed and purified recombinant fusion protein consisting of His-TF and OsWRKY45 efficiently bound to W-box motif-containing probes, but not mutated probes. Increasing amounts of unlabelled probes could weaken OsWRKY45 binding on labelled W-box motif (Figure 8b), suggesting that OsWRKY45 specifically targets to W-box motif within the *OsGELP77* promoter. In addition, we performed ChIP-qPCR assays to evaluate the binding of OsWRKY45 to *OsGELP77* promoter. OsWRKY45 binding was enriched at the three W-box motifs, suggesting that OsWRKY45 bound to the *OsGELP77* promoter in vivo (Figure 8c). Lastly, to determine the effect of OsWRKY45 on the *OsGELP77* expression, we performed transient expression assays in rice protoplast cells using a construct that *OsWRKY45* driven by the *Ubiquitin* promoter as an effector and a construct that the firefly luciferase gene driven by the intact or mutated *OsGELP77* promoter as a reporter. The $P_{OsGELP77}$:LUC construct but not the m$P_{OsGELP77}$:LUC construct resulted in significantly enhanced LUC activity in protoplasts, conforming transcriptional activation for OsWRKY45 toward on *OsGELP77* (Figure 8d). Collectively, these results indicate that OsWRKY45 can directly bind to the promoter of *OsGELP77* to activate its transcription.

OsWRKY45 genetically acts upstream of *OsGELP77*

To determine the genetic epistasis between *OsWRKY45* and *OsGELP77* in the JA-dependent immunity, we crossed the

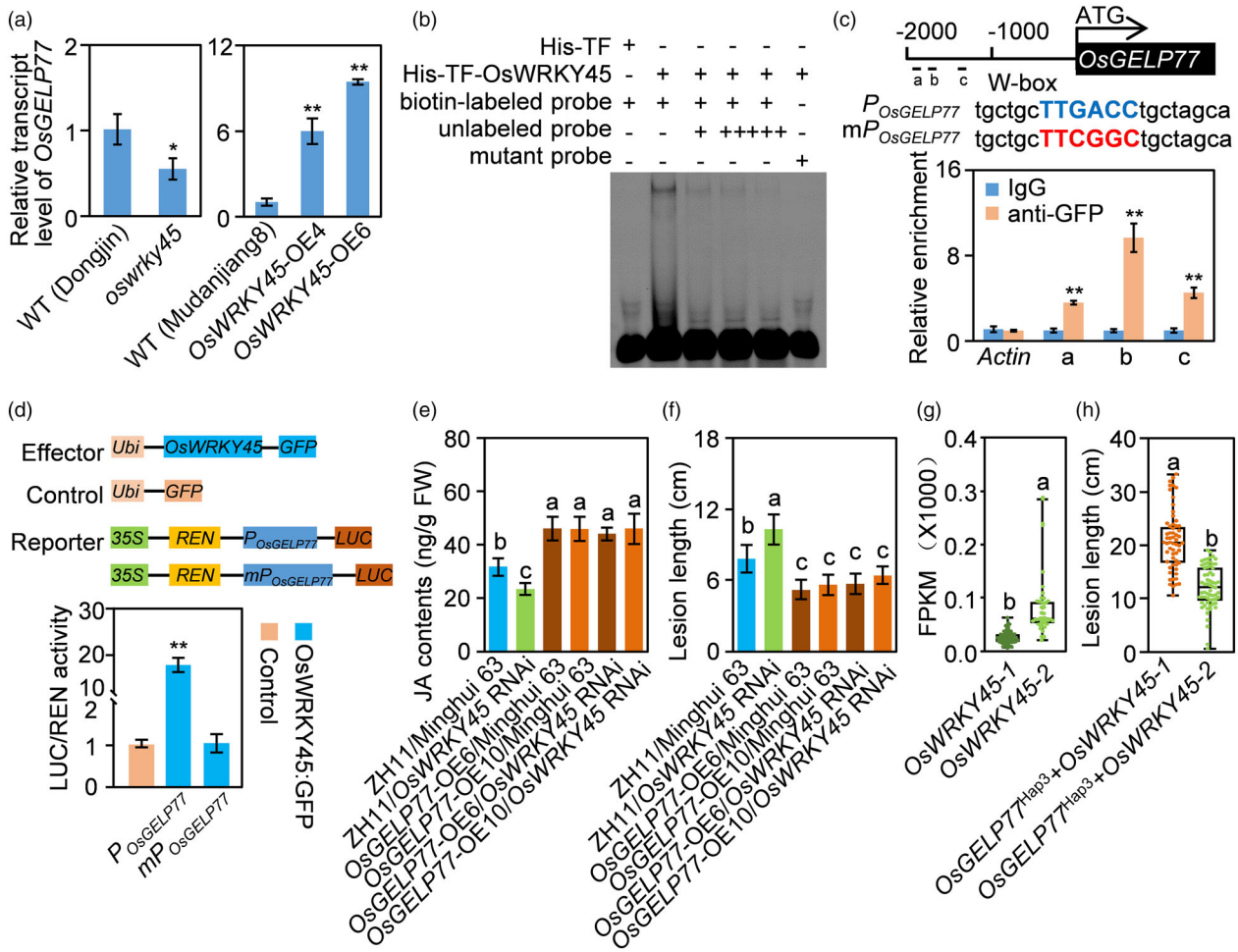

Figure 8 OsWRKY45 genetically acts upstream of *OsGELP77*. (a) *OsGELP77* expression in *OsWRKY45*-OE and *oswrky45* mutant. (b) DNA binding activity assay of OsWRKY45 by EMSA assay. (c) Binding assay of OsWRKY45 to the promoter of *OsGELP77* by ChIP-qPCR in *OsWRKY45*:GFP plants using the anti-GFP antibody. Anti-GFP antibody was used for immunoprecipitation and IgG acted as a control. The blue capital letters indicate the intact W-box, the red capital letters represent the mutated W-box. (d) Activity assay of OsWRKY45 in regulating *OsGELP77* expression. (e) JA contents in the leaves of transgenic plants and the corresponding background. (f) Responses of the transgenic plants and the corresponding background to *Xoo* strain PXO99. Plants were inoculated with *Xoo* at the booting stage. (g) FPKM values of *OsWRKY45-1* and *OsWRKY45-2* in rice leaf. (h) Responses of rice varieties harbouring $OsGELP77^{Hap3}$ and *OsWRKY45-1* or *OsWRKY45-2* to *Xoo* strain PXO99. Plants were inoculated with *Xoo* at the booting stage. Data represent means ± SD. $n = 3$ (a, c, d, e), $n = 30$ (f). Asterisks in (a, c, d) indicate significant differences between transgenic plants and WT or control determined by two-tailed Student's *t*-test at $^{**}P < 0.01$ or $^{*}P < 0.05$. The different letters above each bar in (e, f, g, h) indicate statistically significant differences, as determined by one-way ANOVA analysis followed by Tukey's multiple test ($P < 0.05$).

OsGELP77-OE plant with *OsWRKY45* RNAi line which exhibited susceptible to pathogens in Minghui 63 background. We found overexpression of *OsGELP77* could markedly accumulate JA in *OsWRKY45* RNAi line as that in Minghui 63, although the *OsWRKY45* RNAi line had attenuated JA level relative to the corresponding background (Figure 8e). In agreement, overexpression of *OsGELP77* enhanced rice resistance to *Xoo* in Minghui 63, and could also reverse the susceptibility of *OsWRKY45* RNAi line to *Xoo* (Figure 8f). Collectively, these results support that OsWRKY45 genetically acts upstream of *OsGELP77* modulating disease resistance.

Previously, we have demonstrated that *japonica* rice varieties exclusively carry *OsWRKY45-1*, *indica* rice varieties all carry *OsWRKY45-2*. The major difference in DNA sequences between *OsWRKY45-1* and *OsWRKY45-2* is a TE-siR815b insertion in the first intron of *OsWRKY45-1* (Tao *et al*., 2009; Zhang *et al*., 2016). When evaluating the *OsWRKY45* expression in leaf transcriptomes of 287 rice varieties (Liu *et al*., 2022), we found *OsWRKY45-2* expression was higher than *OsWRKY45-1* (Figure 8g). In agreement, rice varieties harbouring $OsGELP77^{Hap3}$ and *OsWRKY45-2* had significantly shorter lesion lengths compared with those harbouring $OsGELP77^{Hap3}$ and *OsWRKY45-1* after *Xoo* infection (Figure 8h). These results further confirm the OsWRKY45-*OsGELP77* cascade positively triggers rice immunity.

Discussion

In response to pathogen attacks, plants have evolved a wide range of defence strategies to protect themselves, such as activating plant immune signalling networks, reprogramming transcriptional or translational regulatory systems, modulating phytohormone or secondary metabolite homeostasis (Wang *et al*., 2022). In this work, we showed that host rice regulates OsWRKY45-activated *OsGELP77* expression to modulate lipid metabolism, resulting in increased JA accumulation and strengthened JA signal transduction to boost immunity.

OsGELP77 modulates lipid metabolism

Of the 115 GDSL genes in rice, nine of them have been functionally characterized, including that *OsGELP34/RMS2*, *OsGELP110*, and *OsGELP115* control pollen exine development (Zhang *et al*., 2020; Zhao *et al*., 2020b), *OsGELP64/MHZ11* modulates ethylene signalling in roots (Zhao *et al*., 2020a), *OsGELP62/DARX1* and *OsGELP33/DR/BS1/GER1* regulate secondary wall formation and patterning (Riemann *et al*., 2007; Yu *et al*., 2020; Zhang *et al*., 2017a, 2019), *OsGLIP1* and *OsGELP78/OsGLIP2* negatively modify rice immunity (Gao *et al*., 2017), and *OsGELP112/WDL1* affects cutin formation (Park *et al*., 2010). Here, we revealed that a new member, *OsGELP77*, positively regulates rice broad-spectrum resistance and promotes grain yield. Like rice GDSL lipases reported previously, OsGELP77 exhibits lipase activity toward universal substrates such as *p*-nitrophenyl butyrate, *p*-nitrophenyl acetate, *p*-nitrophenyl octanoate, or *p*-nitrophenyl palmitate via the in vitro and in vivo assays (Figure 2e,f). However, the in vivo substrates for OsGELP77 have not yet been identified in this study that is the same as other rice GDSL lipases with substrates unknown. Although lipid profiling has enabled us to compare the abundance of individual lipid species in the *OsGELP77*-OE plant and *osgelp77* mutant, the precise substrates that OsGELP77 catalysed or the biochemical reactions that OsGELP77 involved are still unclear. We speculate that both the technical limitation of mass spectrometry-based lipidomics and broad substrates of GDSL lipases might have effects on disclosing the precise substrates for OsGELP77 (Hu and Zhang, 2018).

Based on mass spectrometry-based lipidomics, 379 individual lipid species belonging to 12 classes of lipids could be identified and quantified in the *OsGELP77* transgenic plants. Seven of the 12 classes of lipids had altered accumulations that PA, PS, FFA, and TAG contents were positively correlated with *OsGELP77* expression, while PG, PI, and DAG contents were negatively correlated with *OsGELP77* expression (Figure 3). The widely altered contents of different classes of lipids in the transgenic plants are possibly related to broad substrates of OsGELP77 because recombinant OsGELP77 could catalyse the hydrolysis of both short-chain substrates (*p*-nitrophenyl butyrate, *p*-nitrophenyl acetate, *p*-nitrophenyl octanoate) and long-chain substrate (*p*-nitrophenyl palmitate). When evaluating lipid profiling, the *OsGELP77* transgenic plants had different kinds of accumulated lipid species compared with such as *OsGLIP1*, *OsGLIP2*, or *OsGELP64/MHZ11* transgenic plants (Gao *et al*., 2017; Zhao *et al*., 2020a), which may the result that these GDSL lipases prefer different substrates *in planta*. In addition, OsGELP110 and OsGELP115 are localized in the peroxisomes and OsGELP33/DR/BS1/GER1 is localized in the Golgi apparatus, the other seven GDSL lipases are all localized in the ER. The different subcellular localization of GDSL lipases may also have effects on lipid metabolism.

OsGELP77 positively regulates rice immunity and yield

Several GDSL lipases have been reported involved in plant defence responses under different manners. *Arabidopsis GLIP1*, *GLIP2*, and *AtGDSL1*, and *Brassica napus BnGDSL1* play positive roles in defence responses (Ding *et al*., 2020; Kwon *et al*., 2009; Lee *et al*., 2009; Oh *et al*., 2005). In contrast, rice *OsGLIP1* and *OsGLIP2* play negative roles in against pathogen attacks (Gao *et al*., 2017). In this study, we proposed that *OsGELP77* is a positive regulator of rice immunity that overexpression of *OsGELP77* significantly increased rice resistance to bacterial pathogens *Xoo* or *Xoc* and fungal pathogen *M. oryzae*, while *OsGELP77* loss-of-function mutants decreased disease resistance to various pathogens (Figure 1). Moreover, OsGELP77 acts as a lipase thus modulates lipid metabolism, which ultimately alters JA homeostasis. As JAs are lipid-derived phytohormones, it is not surprise that overexpression of *OsGELP77* enhanced JA accumulation. The *OsGELP77* overexpressing plants accumulated more JA and had elevated expressions of plant immune regulators, which supports the widely accepted view that JA accumulation or JA signalling activation indicates constitutive defence activation (Yang *et al*., 2013). However, because OsGELP77-modulated lipid metabolism occurred in ER, and JA biosynthesis takes place in chloroplasts and peroxisomes (Wan and Xin, 2022; Yang *et al*., 2013), the direct relationship between OsGELP77-modulated lipid metabolism and OsGELP77-regulated JA accumulation is urgently waiting for exploration in the future.

Similar to OsGLIP1 or OsGLIP2, OsGELP77 possesses lipase activity, however, these three rice GDSL lipases play reverse roles in plant immunity due to their diverse features. Firstly, *OsGELP77* expression was induced in response to pathogen infection, while both *OsGLIP1* and *OsGLIP2* expressions were suppressed against pathogen attacks. Secondly, *OsGELP77* expression was elevated upon treatment of defence signalling molecule JA while not SA, however, *OsGLIP1* and *OsGLIP2* expressions were inhibited after SA treatment. Lastly, OsGELP77 possibly modulated the contents

of lipid species including PA, PG, PI, PS, FFA, DAG, and TAG, while OsGLIP1 and OsGLIP2 largely influence the levels of DGDG and MGDG. Therefore, the different expression patterns of these three rice GDSL genes in response to pathogen attacks and defence signalling molecule treatment, and the difference of native lipid substrates for them may coordinately determine their diverse roles in immunity.

Although *Arabidopsis GLIP1*, *GLIP2*, *AtGDSL1*, and rice *OsGELP77* positively modulate defence response, they regulate plant immunity through regulation of different phytohormone signalling. GLIP1 modulates immunity through feedback regulation of ethylene signalling (Kim *et al*., 2013; Kwon *et al*., 2009). GLIP2 confers pathogen resistance via regulation of auxin signalling (Lee *et al*., 2009). *AtGDSL1*-mediated resistance against pathogens may depend on SA signalling (Ding *et al*., 2020). However, we here revealed that OsGELP77-triggered resistance may largely rely on JA signalling. Except for increased expression of JA biosynthetic genes in the *OsGELP77*-OE plants, there were also reprogrammed expression of key JA signalling genes, such as increased *OsMYC2* and decreased four *OsJAZs* which have been reported playing critical roles in rice immune responses (Sun *et al*., 2022; Uji *et al*., 2016; Yamada *et al*., 2012). Moreover, the assessment of growth inhibition upon exogenous treatment of JA to seedlings of *OsGELP77*-OE plant and *osgelp77* mutant revealed that *OsGELP77* is involved in JA signal transduction (Figure S15). Clearly, these *GDSL* genes stimulate host immune responses through the regulation of different phytohormone signalling. OsGELP77 acts as a lipase involved in lipid metabolism, and JA is a class of lipid-derived phytohormone. Thus, it is logical that OsGELP77 modulates JA accumulation or JA signalling against pathogen attacks. Because OsGELP77 had broad substrates, whether OsGELP77-catalysed lipid metabolism affects the homeostasis or signalling of other phytohormones that in turn boosts rice immunity should be further investigated.

JA has been reported to increase grain yield through regulating spikelet formation and development in rice (Deveshwar *et al*., 2020). Both the *OsGELP77*-OE plant and NIL-*OsGELP77*^{Hap3} line had higher JA accumulation. Therefore, overexpression of *OsGELP77* and pyramiding an elite haplotype *OsGELP77*^{Hap3} all could promote grain yield. The high proportion of *OsGELP77*^{Hap3} may be attributed to the advocated breeding strategy. In the present study, Minghui 63 presents *OsGELP77*^{Hap3} and Zhenshan 97 presents *OsGELP77*^{Hap1}, Shanyou 63, an elite mega rice hybrid in China, is derived from the cross by Minghui 63 and Zhenshan 97. Thus, we could not exclude the contribution of *OsGELP77*^{Hap3} to heterosis. *OsGELP77* positively regulates broad-spectrum disease resistance and promotes yield, thus, it is not surprise that *OsGELP77*^{Hap3} has been widely used to breed hybrid rice.

OsGELP77 is a disease-resistance QTL

With the accessibility of huge amounts of genome-wide SNPs and InDels and large amounts of high-throughput phenotypic data against different pathogens for a large number of rice accessions, a lot of resistance QTL have been identified based on genome-wide association studies (GWAS) or linkage QTL mapping in rice (Deng *et al*., 2020; Kou *et al*., 2010; Liu *et al*., 2021). However, a great amount of the causal QTL have not been functionally characterized. Contrary to QTL identification by forward genetics through GWAS and QTL mapping, we here by reverse genetics revealed that *OsGELP77* is a disease-resistance QTL which is supported by the following evidence: (1) *OsGELP77* co-located with several disease-resistance QTL that were derived using different rice accessions (Figure S18); (2) *OsGELP77* colocalized with the curve peak of resistance QTL against both bacterial pathogen and fungal pathogen by QTL mapping using a previously developed RIL population (Figure 7a); and (3) *OsGELP77* acts as a disease-resistance QTL which was experimentally validated by evaluating the defence response of the constructed a NIL-*OsGELP77*^{Hap3} (Figure 7).

OsWRKY45 activates *OsGELP77* triggering immunity

OsWRKY45 positively regulates broad-spectrum resistance to bacterial and fungal pathogens via SA- and JA-dependent signalling pathways (Shimono *et al*., 2012; Tao *et al*., 2009). Transcription factors IPA1 and OsARF8 could activate and repress the expression of *OsWRKY45*, respectively (Feng *et al*., 2022; Wang *et al*., 2018). Moreover, OsWRKY45 could activate its downstream target genes including *OsWRKY13*, *OsWRKY62*, and *OsNAC4* (Cheng *et al*., 2015; Nakayama *et al*., 2013). The deciphered transcriptional cascades mainly explain the SA-dependent signalling pathway for OsWRKY45-mediated broad-spectrum resistance. Here, we uncover the JA-dependent signalling pathway for OsWRKY45-mediated rice resistance that OsWRKY45 directly targets and activates *OsGELP77* expression to modulate lipid metabolism, resulting in increased JA accumulation and strengthened JA signal transduction. The biochemical assays demonstrate that OsWRKY45 binds to *OsGELP77* promoter and activates its transcription, the genetic assays confirm that OsWRKY45 genetically acts upstream of *OsGELP77* and the OsWRKY45-*OsGELP77* cascade confers rice immunity via JA-dependent signalling pathway (Figure 8). Published data and present results jointly demonstrate that OsWRKY45 activates different target genes to modulate SA and JA signalling pathways to trigger rice immunity.

In summary, our findings identify that *OsGELP77*, a QTL contributing to broad-spectrum disease resistance and yield, encodes a GDSL-type lipase which modulates lipid metabolism to promote JA accumulation, promoting both immunity and yield. OsWRKY45 can directly bind to the promoter of *OsGELP77* and activate its expression, leading to an enhanced JA signalling pathway which triggers rice immunity. The elite haplotype *OsGELP77*^{Hap3} is considered to be a valuable resource for breeding disease-resistant and high-yielding rice.

Materials and methods

Plant materials and growth conditions

Rice (*Oryza sativa* ssp. *Geng*) cultivar Zhonghua 11 (ZH11) and the transgenic rice in ZH11 genetic background were used for experiments. The *OsGELP77*-overexpressing (*OsGELP77*-OE) plants and *osgelp77* knockout mutants were generated in ZH11 as described below. The *coi1-13* mutants were generated in Nip background (Yang *et al*., 2012). The *osmyc2* mutants were generated in ZH11 background (Qiu *et al*., 2022). The *OsWRKY45*-OE, *OsWRKY45*-RNAi, *OsWRKY45*:GFP, and *oswrky45* transgenic plants were generated previously in different background (Cheng *et al*., 2015; Tao *et al*., 2009).

Rice materials were planted in the Experimental Station of Huazhong Agricultural University in normal rice growing seasons (from May to October) under natural conditions (Chu *et al*., 2022).

Generation of constructs and transgenic plants

The full-length cDNA of *OsGELP77* without stop codon was amplified from cDNA of ZH11 leaves by PCR using the specific

primers (Table S3), and then the amplified PCR products were cloned into the pU1301 vector via restriction–ligation method to generate the *OsGELP77*-OE construct (Yuan *et al*., 2010). CRISPR/Cas9-mediated mutagenesis strategy was used to knock out *OsGELP77* gene. Two 20-bp sgRNA designed using the web tool CRISPR-P (http://crispr.hzau.edu.cn/CRISPR2/) which specifically target the first exon of *OsGELP77*, were constructed on the sgRNA expression cassettes of OsU6a and OsU3 by overlapping PCR, and then these two cassettes were subcloned into the pYLCRISPR/Cas9 expression vector via Gibson Assembly cloning method to generate the *OsGELP77* knockout construct (Ma *et al*., 2015). The *OsGELP77* promoter was amplified from DNA of ZH11 leaves by PCR using the specific primers (Table S3), and then the amplified PCR products were inserted upstream of the reporter *β-glucuronidase* (*GUS*) gene into the DX2181 vector via over-lapping PCR method to generate the *OsGELP77pro:GUS* construct (Yang *et al*., 2022). The insertion fragments of all the constructs were verified by DNA sequencing using the vector-specific primers (Table S3). All the constructs were transformed into *Agrobacterium tumefaciens* strain EHA105, which were then transformed into rice calli from mature embryos of ZH11. Transgenic rice plants were generated by *Agrobacterium*-mediated transformation (Chu *et al*., 2022). The positive lines of *OsGELP77*-OE plants were verified by PCR using the gene-specific primer and vector-specific primer. The homozygous *osgelp77* mutants were confirmed by sequencing the genome DNA of *OsGELP77*.

Pathogen inoculation

For bacterial pathogen inoculation assay, eight to ten uppermost fully expanded leaves of each plant were inoculated with *Xoc* at the tillering stage or *Xoo* at the booting stage. Briefly, *Xoc* or *Xoo* stocks were streaked on nutrient agar medium (3 g/L beef extract, 5 g/L polypeptone, 1 g/L yeast extract, 10 g/L sucrose, and 20 g/L agar) and incubated at 28 °C for 2 days (Yang *et al*., 2022). Bacterial cells were collected from the agar medium, suspended in sterilized water, and adjusted to an optical density of 0.5 at 600 nm. Rice leaves were inoculated with *Xoc* by the penetration method or *Xoo* by the leaf-clipping method (Hui *et al*., 2019). *Xoc* or *Xoo* strains isolated from different rice-growing regions show virulence on rice variety ZH11 and Zhenshan 97 (Hui *et al*., 2019). *Xoc* used in this study included four strains (RH3, HNB8-47, GX01, and RS105). *Xoo* used in this study included five strains (PXO61, PXO99, PXO341, PXO71, and PXO347). Disease was assessed by counting colony-forming units every 4 days after *Xoc* or *Xoo* inoculation and measuring the lesion length of rice leaves 14 days post bacterial pathogen inoculation (Yuan *et al*., 2016).

For the fungal pathogen inoculation assay, rice leaves were inoculated with *M. oryzae* at the tillering stage. Briefly, *M. oryzae* isolate 99-20-2 was cultured on oatmeal tomato agar medium (15% tomato juice, 40 g/L oatmeal, and 20 g/L agar) at 28 °C for 5 days. Conidia were collected from the medium, suspended in sterilized water containing 0.05% Tween-20, and adjusted to an optical density of 5.0×10^5 spores per millilitre. Rice leaves were inoculated with *M. oryzae* by the punch inoculation method (Chu *et al*., 2022). Disease was scored by measuring the lesion length and quantifying fungal biomass at 7 days after *M. oryzae* inoculation. The fungal biomass in infected rice leaves was analysed using the threshold cycle value of *M. oryzae Pot2* DNA against the cycle value of rice genomic *ubiquitin* DNA (Chu *et al*., 2022).

MeJA treatment and hormone quantification

Rice seeds were surface-sterilized with 75% ethanol and 2.5% sodium hypochlorite and pregerminated on 1/2 Murashige and Skoog medium for 2 days. The identically sprouted seeds were transplanted on Murashige and Skoog medium supplemented with different concentrations of MeJA for 7 days. The lengths of primary roots and shoots were measured and seedlings were photographed.

Rice seedlings growing in a controlled growth greenhouse at the 5-leaf stage were sprayed with 250 μM MeJA which was dissolved in 0.05% (v/v) methanol and 0.05% (v/v) Tween 20 or mock control solution containing 0.05% (v/v) methanol and 0.05% (v/v) Tween 20 until uniformly wet. The treated rice plants were kept in sealed plastic shade for 2 days, and then inoculated with *Xoc* or *Xoo*.

For JA and SA quantification, leaves of rice growing in the paddy field at the tillering stage were sampled and ground in liquid nitrogen. About 100 mg powder of each sample was mixed with the extraction buffer (methanol:water:acetic acid = 40:9:1, v/v/v) that supplemented with stable isotope-labelled internal standards, vigorously shaken in the dark at 4 °C for 16 h, and then centrifuged at 4 °C for 20 min. The supernatants were filtered through a syringe-facilitated nylon filter, dried by evaporation under the flow of nitrogen gas, and finally dissolved in methanol. JA and SA were quantified by an ultrafast liquid chromatography coupled to electrospray ionization tandem mass spectrometry (UFLC-ESI-MS/MS) in an ABI 4000 Q-TRAR system (Applied Biosystems) according to a previously reported method (Huang *et al*., 2018).

Gene expression analysis

Total RNA was extracted from different rice tissues using Trizol reagent (Invitrogen). About 5 μg total RNA was pre-treated with RNase-free DNase I (Invitrogen) to eliminate potentially contaminating DNA, and then was reverse-transcribed into cDNA using oligo$(dT)_{15}$ primer and M-MLV reverse transcriptase (Promega) according to the manufacturer's protocol. For gene expression analysis, quantitative real-time PCR (RT-qPCR) was performed using MonAmp™ ChemoHS qPCR Mix (Monad, China) in the ABI QuantStudio™ (Applied Biosystems). RT-qPCR was carried out using gene-specific primers (Table S4) which were designed using the Primer Express v3.0 software (Applied Biosystems). The rice *actin* gene was used to standardize relative RNA measures as inner control (Chu *et al*., 2022). Each RT-qPCR assay was biologically repeated at least twice with similar results, with each repetition having three technical replicates (Yuan *et al*., 2016). The Student's *t*-test was used for the RT-qPCR analysis.

Transcriptome analysis

Rice leaves at the booting stage of the *osgelp77* mutant and wild type were sampled with three biological replicates for whole transcriptome analysis. The assays including library construction and Illumina HiSeq4000 platform-based sequencing were carried out by Novogene (Beijing, China). The analysis including read quality evaluation, clean reads mapping, transcript abundance measurement, and differential expression analysis was conducted at the Galaxy platform (https://usegalaxy.org/) according to the workflow. The gene with relative expression $\log_2FC \geq 1$ or $\log_2FC \leq -1$ and the false discovery rate (FDR) < 0.05 considered as differentially expressed genes (Hong *et al*., 2015). Goatools was used for the Gene Ontology (GO) analysis and KOBAS was

used for the Kyoto Encyclopedia of Genes and Genomes (KEGG) analysis with an adjusted *P* value cutoff of 0.05.

Transient expression assays in rice protoplasts

The *OsGELP77* promoter (2 kb upstream of the translational ATG start codon) was amplified by PCR using gene-specific primers (Table S3), cloned into the pGreen II 0800 vector to generate the $P_{OsGELP77}$:LUC construct as reporter. The three W-box motifs of *OsGELP77* promoter were mutated using the GeneTailor Site-Directed Mutagenesis System (Invitrogen Life Technologies) to generate the m$P_{OsGELP77}$:LUC construct. The coding sequence of *OsWRKY45* was amplified with gene-specific primers (Table S3), then cloned into the pU1301 vector to generate the Ubi:OsWRKY45 construct as effector. The corresponding reporter and effector constructs were co-transfected into rice protoplasts as described previously (Ke *et al*., 2020). After culturing for 16 h in dark at 25 °C, the transfected protoplasts were gathered by centrifugation at 100 ***g*** for 8 min. The luciferase activities were measured using Dual Luciferase Reporter Assay System (Promega) by a Spark Multimode Microplate Reader (Tecan, Switzerland) according to the manufacturer's instructions. The relative reporter gene expression levels were expressed as the ratio of firefly luciferase (LUC) to renilla luciferase (REN).

Subcellular localization assays

The full-length *OsGELP77* cDNA was amplified by PCR using the specific primers (Table S3), and then the amplified PCR products were cloned into the pRTVnGFP vector (He *et al*., 2018), to generate the *GFP:OsGELP77* construct where *OsGELP77* was in-frame and downstream of the green fluorescent protein (*GFP*) that driven by the maize *Ubiquitin* promoter. After sequencing using the gene-specific primer, the GFP:OsGELP77 construct was transiently introduced into rice protoplasts which were isolated from 12-day-old green rice leaf sheaths via PEG-mediated transformation (Yang *et al*., 2022). The protoplasts were incubated at 28 °C for 12 h, and then were visualized for fluorescent signals by a Leica Microsystem (LAS AF, Germany) according to a previously reported protocol (Yang *et al*., 2022). Alternatively, after incubation for 12 h, the protoplasts were treated with 100 nM flg22 for 2 h, and then visualized for fluorescent signals.

Chromatin immunoprecipitation (ChIP)-qPCR

The ChIP assays were performed as described previously (Ke *et al*., 2020). In brief, chromatin was extracted from the *OsWRKY45:GFP* seedlings (Cheng *et al*., 2015), and fragmented to 200–400 bp via ultrasound. The OsWRKY45:GFP protein bonding DNAs were enriched using protein A Dynabeads (Invitrogen) coupling with anti-GFP antibody or IgG as control at 4 °C overnight. After abundant washing and de-crosslinking, the input and precipitated DNA samples were amplified by qPCR using gene-specific primers (Table S3).

Electrophoretic mobility shift assays (EMSA)

EMSA assays were performed using Light Shift Chemiluminescent EMSA Kit (Thermo Scientific), as described previously (Ke *et al*., 2020). In brief, the synthesized 5-carboxyfluorescein biotin-labelled probes were incubated with purified His-TF-OsWRKY45 recombinant proteins for 30 min at room temperature. The equal and increasing amounts of unlabelled probes were mixed with labelled probes for competition reaction. The mutant probes were used as negative control. The protein-DNA complex was separated on a 6% PAGE gel for 3 h at 4 °C in the dark. Gels were photographed using FLA-5100 (FUJIFILM, Japan).

Histochemical GUS staining

Histochemical GUS staining was performed according to a previously reported method (Yuan *et al*., 2009). In brief, rice tissues including nodes, roots, leaves, sheaths, and panicles were immersed in GUS staining solution (50 mM of sodium phosphate buffer at pH 7.0, 10 mM of EDTA, 0.1% Triton X-100, 1 mg/mL of X-Gluc, 100 mg/mL of chloramphenicol, 1 mM of potassium ferrocyanide, 1 mM of potassium ferricyanide, and 20% methanol), infiltrated under a vacuum for 30 min, and incubated at 37 °C for 24 h. Then, the stained rice tissues were immersed in a fixation solution (50% ethanol, 3.7% formaldehyde, and 5% acetic acid) at 25 °C for 24 h. Various rice tissues were photographed using a stereo microscope (Leica M205 FCA, Germany).

Recombinant protein purification and lipase activity assay

The full-length OsGELP77 cDNA without the N-terminal signal peptide was amplified using the specific primers (Table S3), then the amplified PCR products were cloned into the pGEX-6p-1 vector (GE Healthcare). Simultaneously, OsGELP77^{4A} where the four invariant key catalytic residues were mutated to alanine using overlapping-PCR method was cloned into the same vector. The constructs were transformed into *Escherichia coli* BL21 (DE3) cells. The expression of the recombinant OsGELP77ΔSP or OsGELP77^{4A}ΔSP proteins was induced using 1 mM isopropylthio-β-galactoside at 16 °C. After induction for 20 h, cells were collected, suspended in PBS buffer, and sonicated. The recombinant proteins were purified using GST-tag beads (GE Healthcare) according to the manufacturer's instructions and confirmed by SDS-PAGE gel. The recombinant His-TF-OsWRKY45 protein and the control His-TF protein were prokaryote-expressed and purified using Ni Sepharose 6 fast Flow (GE Healthcare), as described previously (Cheng *et al*., 2015).

Lipase activity was measured according to a previously reported method (Gao *et al*., 2017). In brief, *p*-nitrophenyl butyrate, *p*-nitrophenyl acetate, *p*-nitrophenyl octanoate, or *p*-nitrophenyl palmitate was dissolved in a buffer containing 0.5 M HEPES, reaching a final concentration of 1 mM. Aliquots of the recombinant proteins were incubated with the substrates at 30 °C for 90 min. Absorbance was quantified spectrometrically at 405 nm every 5 min using a Spark™ Multimode Microplate Reader (Tecan, Switzerland).

Lipidomics analysis

The lipidomics analysis of rice leaves was performed according to previously reported methods (Chen *et al*., 2013; Gao *et al*., 2017). In brief, rice leaves growing in the paddy field at the tillering stage were sampled and ground in liquid nitrogen. About 50 mg powder of each sample was mixed with 1 mL methanol, 1 mL chloroform, and 0.8 mL ultra-purified water, and vigorously shaken for 10 min for lipid extraction. Following centrifugation, the organic phase was orderly treated with chloroform and 1 M KCl to purify lipid. The organic solution was filtered, then dried under the flow of nitrogen gas, and finally dissolved in chloroform. Lipid species quantification was conducted using a liquid chromatography-electrospray ionization triple quadrupole mass spectrometry (LC-ESI-MS/MS) system (LC, Shim-pack UFLC SHIMADZU CBM30A; MS, ABI 6500 QTRAP) by Metware

(Wuhan, China). Individual lipid species were analysed based on metabolite structure referring to public mass spectrometry databases including Metware-made database (Chen *et al.*, 2013), Metlin (http://metlin.scripps.edu/), and MassBank (http://www.massbank.jp/).

Haplotype analysis and multiple sequence alignments

The genomic sequence of *OsGELP77* in 2178 rice accessions was acquired from RiceVarMap v2.0 (http://ricevarmap.ncpgr.cn/). Haplotypes of the accessions were analysed from InDels and SNPs in *OsGELP77* promoter. Protein sequences of functionally characterized plant GDSL proteins were retrieved from NCBI. Multiple sequence alignments of protein were analysed using Clustal Omega (www.clustal.org/omega).

Co-mapping *OsGELP77* and resistance QTL

A rice recombinant inbred line (RIL) population consisting of 241 lines developed from a cross between resistant Minghui 63 and susceptible Zhenshan 97 was used to analyse co-mapping *OsGELP77* and resistance QTL (Kou *et al.*, 2010). The RIL population has been previously used to identify the quantitative disease resistance for bacterial pathogen *Xoo* and fungal pathogen *M. oryzae* (Chen *et al.*, 2003; Kou *et al.*, 2010). A molecular linkage map containing 221 simple-sequence repeats markers that covering the whole rice genome was previously developed with the RIL population for QTL mapping. *OsGELP77* was mapped on the molecular linkage map developed from the RIL population using PCR-based derived cleaved amplification polymorphism sequence (dCAPS) marker which was designed using dCAPS Finder (http://helix.wustl.edu/dcaps/dcaps.html). Mapmaker/Exp 3.0 was used for linkage analysis and Windows QTL Cartographer 2.5 was used for QTL analysis (Kou *et al.*, 2010).

Agronomic traits analysis

All rice plants were cultivated in three replicates at three different plots under natural field conditions in normal rice growing season. Agronomic traits including plant height, tiller number, flag leaf length, flag leaf width, panicle length, productive panicles per plant, grain length, grain width, grain thickness, primary branch number, and 1000-grain weight were measured at the ripening stage. Of which, traits such as grain length, grain width, grain thickness, primary branch number, and 1000-grain weight were measured by the high-throughput rice phenotyping facility (Yang *et al.*, 2014).

Statistical analysis

Statistical parameters are reported in the figures and figure legends. The differences between samples were analysed for statistical significance using ANOVA or Student's *t*-test.

Acknowledgements

We are grateful to Prof. Donglei Yang at Nanjing Agricultural University for providing *coi1-13* mutant and Prof. Yanjun Kou at China National Rice Research Institute for providing *osmyc2* mutant. This work was supported by grants from the STI 2030-Major Projects (2022ZD0400201), the National Natural Science Foundation of China (31821005, 32172421), the Major Project of Hubei Hongshan Laboratory (2022hszd016), the earmarked fund for the China Agriculture Research System (CARS-01-01), the Fundamental Research Funds for the Central Universities (2662023PY006) and the open funds of the National Key Laboratory of Crop Genetic Improvement.

Conflict of interest

The authors declare no conflict of interest.

Author contributions

MY, MZ, and DC designed the experiments, MZ, DC, and JT performed the experiments, JC, KX, and YH assisted the experiments, MZ and DC analysed the data, MY wrote and revised the manuscript.

Data availability statement

The RNA-seq data from this study is deposited to NCBI Sequence Read Archive (BioProject ID: PRJNA895969).

References

Akoh, C.C., Lee, G.C., Liaw, Y.C., Huang, T.H. and Shaw, J.F. (2004) GDSL family of serine esterases/lipases. *Prog. Lipid Res.* **43**, 534–552.

Brick, D.J., Brumlik, M.J., Buckley, J.T., Cao, J.X., Davies, P.C., Misra, S., Tranbarger, T.J. *et al.* (1995) A new family of lipolytic plant enzymes with members in rice, arabidopsis and maize. *FEBS Lett.* **377**, 475–480.

Brodersen, P., Petersen, M., Bjørn Nielsen, H., Zhu, S., Newman, M.A., Shokat, K.M., Rietz, S. *et al.* (2006) Arabidopsis MAP kinase 4 regulates salicylic acid- and jasmonic acid/ethylene-dependent responses via EDS1 and PAD4. *Plant J.* **47**, 532–546.

Cai, Q., Yuan, Z., Chen, M., Yin, C., Luo, Z., Zhao, X., Liang, W. *et al.* (2014) Jasmonic acid regulates spikelet development in rice. *Nat. Commun.* **5**, 3476.

Campos, M.L., Kang, J.H. and Howe, G.A. (2014) Jasmonate-triggered plant immunity. *J. Chem. Ecol.* **40**, 657–675.

Chen, H., Wang, S., Xing, Y., Xu, C., Hayes, P.M. and Zhang, Q. (2003) Comparative analyses of genomic locations and race specificities of loci for quantitative resistance to *Pyricularia grisea* in rice and barley. *Proc. Natl. Acad. Sci. U. S. A.* **100**, 2544–2549.

Chen, W., Gong, L., Guo, Z., Wang, W., Zhang, H., Liu, X., Yu, S. *et al.* (2013) A novel integrated method for large-scale detection, identification, and quantification of widely targeted metabolites: application in the study of rice metabolomics. *Mol. Plant*, **6**, 1769–1780.

Cheng, H., Liu, H., Deng, Y., Xiao, J., Li, X. and Wang, S. (2015) The WRKY45-2 WRKY13 WRKY42 transcriptional regulatory cascade is required for rice resistance to fungal pathogen. *Plant Physiol.* **167**, 1087–1099.

Chepyshko, H., Lai, C.P., Huang, L.M., Liu, J.H. and Shaw, J.F. (2012) Multifunctionality and diversity of GDSL esterase/lipase gene family in rice (*Oryza sativa* L. *japonica*) genome: new insights from bioinformatics analysis. *BMC Genomics*, **13**, 309.

Chu, C., Huang, R., Liu, L., Tang, G., Xiao, J., Yoo, H. and Yuan, M. (2022) The rice heavy-metal transporter OsNRAMP1 regulates disease resistance by modulating ROS homoeostasis. *Plant Cell Environ.* **45**, 1109–1126.

Deng, H., Liu, H., Li, X., Xiao, J. and Wang, S. (2012) A CCCH-type zinc finger nucleic acid-binding protein quantitatively confers resistance against rice bacterial blight disease. *Plant Physiol.* **158**, 876–889.

Deng, Y., Ning, Y., Yang, D.L., Zhai, K., Wang, G.L. and He, Z. (2020) Molecular basis of disease resistance and perspectives on breeding strategies for resistance improvement in crops. *Mol. Plant* **13**, 1402–1419.

Deveshwar, P., Prusty, A., Sharma, S. and Tyagi, A.K. (2020) Phytohormone-mediated molecular mechanisms involving multiple genes and QTL govern grain number in rice. *Front. Genet.* **11**, 586462.

Ding, L.N., Li, M., Guo, X.J., Tang, M.Q., Cao, J., Wang, Z., Liu, R. *et al.* (2020) *Arabidopsis* GDSL1 overexpression enhances rapeseed *Sclerotinia sclerotiorum* resistance and the functional identification of its homolog in *Brassica napus*. *Plant Biotechnol. J.* **18**, 1255–1270.

Feng, Q., Wang, H., Yang, X.M., Hu, Z.W., Zhou, X.H., Xiang, L., Xiong, X.Y. *et al*. (2022) Osa-miR160a confers broad-spectrum resistance to fungal and bacterial pathogens in rice. *New Phytol.* **236**, 2216–2232.

Gao, M., Yin, X., Yang, W., Lam, S.M., Tong, X., Liu, J., Wang, X. *et al*. (2017) GDSL lipases modulate immunity through lipid homeostasis in rice. *PLoS Pathog.* **13**, e1006724.

Ghorbel, M., Brini, F., Sharma, A. and Landi, M. (2021) Role of jasmonic acid in plants: the molecular point of view. *Plant Cell Rep.* **40**, 1471–1494.

He, F., Zhang, F., Sun, W., Ning, Y. and Wang, G.L. (2018) A versatile vector toolkit for functional analysis of rice genes. *Rice* **11**, 27.

Hong, H., Liu, Y., Zhang, H., Xiao, J., Li, X. and Wang, S. (2015) Small RNAs and gene network in a durable disease resistance gene-mediated defense responses in rice. *PLoS One*, **10**, e0137360.

Hou, Y., Wang, Y., Tang, L., Tong, X., Wang, L., Liu, L., Huang, S. *et al*. (2019) SAPK10-mediated phosphorylation on WRKY72 releases its suppression on jasmonic acid biosynthesis and bacterial blight resistance. *iScience* **16**, 499–510.

Hu, T. and Zhang, J.L. (2018) Mass-spectrometry-based lipidomics. *J. Sep. Sci.* **41**, 351–372.

Huang, X., Kurata, N., Wei, X., Wang, Z.X., Wang, A., Zhao, Q., Zhao, Y. *et al*. (2012) A map of rice genome variation reveals the origin of cultivated rice. *Nature* **490**, 497–501.

Huang, X., Yang, S., Gong, J., Zhao, Y., Feng, Q., Gong, H., Li, W. *et al*. (2015) Genomic analysis of hybrid rice varieties reveals numerous superior alleles that contribute to heterosis. *Nat. Commun.* **6**, 6258.

Huang, R., Li, Y., Tang, G., Hui, S., Yang, Z., Zhao, J., Liu, H. *et al*. (2018) Dynamic phytohormone profiling of rice upon rice black-streaked dwarf virus invasion. *J. Plant Physiol.* **228**, 92–100.

Hui, S., Shi, Y., Tian, J., Wang, L., Li, Y., Wang, S. and Yuan, M. (2019) TALE-carrying bacterial pathogens trap host nuclear import receptors for facilitation of infection of rice. *Mol. Plant Pathol.* **20**, 519–532.

Ke, Y., Liu, H., Li, X., Xiao, J. and Wang, S. (2014) Rice *OsPAD4* functions differently from Arabidopsis *AtPAD4* in host-pathogen interactions. *Plant J.* **78**, 619–631.

Ke, Y., Yuan, M., Liu, H., Hui, S., Qin, X., Chen, J., Zhang, Q. *et al*. (2020) The versatile functions of OsALDH2B1 provide a genic basis for growth-defense trade-offs in rice. *Proc. Natl. Acad. Sci. U. S. A.* **117**, 3867–3873.

Kim, H.G., Kwon, S.J., Jang, Y.J., Nam, M.H., Chung, J.H., Na, Y.C., Guo, H. *et al*. (2013) GDSL LIPASE1 modulates plant immunity through feedback regulation of ethylene signaling. *Plant Physiol.* **163**, 1776–1791.

Kim, C.K., Seol, Y.J., Lee, D.J., Lee, J.H., Lee, T.H. and Park, D.S. (2014) RiceQTLPro: an integrated database for quantitative trait loci marker mapping in rice plant. *Bioinformation*, **10**, 664–666.

Kou, Y., Li, X., Xiao, J. and Wang, S. (2010) Identification of genes contributing to quantitative disease resistance in rice. *Sci. China Life Sci.* **53**, 1263–1273.

Kwon, S.J., Jin, H.C., Lee, S., Nam, M.H., Chung, J.H., Kwon, S.I., Ryu, C.M. *et al*. (2009) GDSL lipase-like 1 regulates systemic resistance associated with ethylene signaling in *Arabidopsis*. *Plant J.* **58**, 235–245.

Lai, C.P., Huang, L.M., Chen, L.O., Chan, M.T. and Shaw, J.F. (2017) Genome-wide analysis of GDSL-type esterases/lipases in *Arabidopsis*. *Plant Mol. Biol.* **95**, 181–197.

Lavell, A.A. and Benning, C. (2019) Cellular organization and regulation of plant glycerolipid metabolism. *Plant Cell Physiol.* **60**, 1176–1183.

Lee, D.S., Kim, B.K., Kwon, S.J., Jin, H.C. and Park, O.K. (2009) *Arabidopsis* GDSL lipase 2 plays a role in pathogen defense via negative regulation of auxin signaling. *Biochem. Biophys. Res. Commun.* **379**, 1038–1042.

Liu, Z., Zhu, Y., Shi, H., Qiu, J., Ding, X. and Kou, Y. (2021) Recent progress in rice broad-spectrum disease resistance. *Int. J. Mol. Sci.* **22**, 11658.

Liu, C., Zhu, X., Zhang, J., Shen, M., Chen, K., Fu, X., Ma, L. *et al*. (2022) eQTLs play critical roles in regulating gene expression and identifying key regulators in rice. *Plant Biotechnol. J.* **20**, 2357–2371.

Ma, X., Zhang, Q., Zhu, Q., Liu, W., Chen, Y., Qiu, R., Wang, B. *et al*. (2015) A robust CRISPR/Cas9 system for convenient, high-efficiency multiplex genome editing in monocot and dicot plants. *Mol. Plant*, **8**, 1274–1284.

Mei, C., Qi, M., Sheng, G. and Yang, Y. (2006) Inducible overexpression of a rice allene oxide synthase gene increases the endogenous jasmonic acid level, *PR* gene expression, and host resistance to fungal infection. *Mol. Plant Microbe Interact.* **19**, 1127–1137.

Nakayama, A., Fukushima, S., Goto, S., Matsushita, A., Shimono, M., Sugano, S., Jiang, C.J. *et al*. (2013) Genome-wide identification of WRKY45-regulated genes that mediate benzothiadiazole-induced defense responses in rice. *BMC Plant Biol.* **13**, 150.

Neves Petersen, M.T., Fojan, P. and Petersen, S.B. (2001) How do lipases and esterases work: the electrostatic contribution. *J. Biotechnol.* **85**, 115–147.

Oh, I.S., Park, A.R., Bae, M.S., Kwon, S.J., Kim, Y.S., Lee, J.E., Kang, N.Y. *et al*. (2005) Secretome analysis reveals an *Arabidopsis* lipase involved in defense against *Alternaria brassicicola*. *Plant Cell* **17**, 2832–2847.

Park, J.J., Jin, P., Yoon, J., Yang, J.I., Jeong, H.J., Ranathunge, K., Schreiber, L. *et al*. (2010) Mutation in *Wilted Dwarf and Lethal 1* (*WDL1*) causes abnormal cuticle formation and rapid water loss in rice. *Plant Mol. Biol.* **74**, 91–103.

Qiu, J., Xie, J., Chen, Y., Shen, Z., Shi, H., Naqvi, N.I., Qian, Q. *et al*. (2022) Warm temperature compromises JA-regulated basal resistance to enhance *Magnaporthe oryzae* infection in rice. *Mol. Plant* **15**, 723–739.

Riemann, M., Gutjahr, C., Korte, A., Riemann, M., Danger, B., Muramatsu, T., Bayer, U. *et al*. (2007) *GER1*, a GDSL motif-encoding gene from rice is a novel early light- and jasmonate-induced gene. *Plant Biol.* **9**, 32–40.

Shah, J. (2005) Lipids, lipases, and lipid-modifying enzymes in plant disease resistance. *Annu. Rev. Phytopathol.* **43**, 229–260.

Shen, G., Sun, W., Chen, Z., Shi, L., Hong, J. and Shi, J. (2022) Plant GDSL esterases/lipases: evolutionary, physiological and molecular functions in plant development. *Plan. Theory* **11**, 468.

Shimono, M., Koga, H., Akagi, A., Hayashi, N., Goto, S., Sawada, M., Kurihara, T. *et al*. (2012) Rice WRKY45 plays important roles in fungal and bacterial disease resistance. *Mol. Plant Pathol.* **13**, 83–94.

Sun, B., Shang, L., Li, Y., Zhang, Q., Chu, Z., He, S., Yang, W. *et al*. (2022) Ectopic expression of OsJAZs alters plant defense and development. *Int. J. Mol. Sci.* **23**, 4581.

Tao, Z., Liu, H., Qiu, D., Zhou, Y., Li, X., Xu, C. and Wang, S. (2009) A pair of allelic WRKY genes play opposite roles in rice-bacteria interactions. *Plant Physiol.* **151**, 936–948.

Uji, Y., Taniguchi, S., Tamaoki, D., Shishido, H., Akimitsu, K. and Gomi, K. (2016) Overexpression of *OsMYC2* results in the up-regulation of early JA-responsive genes and bacterial blight resistance in rice. *Plant Cell Physiol.* **57**, 1814–1827.

Wan, S. and Xin, X.F. (2022) Regulation and integration of plant jasmonate signaling: a comparative view of monocot and dicot. *J. Genet. Genomics*, **49**, 704–714.

Wang, J., Yu, H., Xie, W., Xing, Y., Yu, S., Xu, C., Li, X. *et al*. (2010) A global analysis of QTLs for expression variations in rice shoots at the early seedling stage. *Plant J.* **63**, 1063–1074.

Wang, J., Zhou, L., Shi, H., Chern, M., Yu, H., Yi, H., He, M. *et al*. (2018) A single transcription factor promotes both yield and immunity in rice. *Science* **361**, 1026–1028.

Wang, Y., Pruitt, R.N., Nürnberger, T. and Wang, Y. (2022) Evasion of plant immunity by microbial pathogens. *Nat. Rev. Microbiol.* **20**, 449–464.

Xie, W., Wang, G., Yuan, M., Yao, W., Lyu, K., Zhao, H., Yang, M. *et al*. (2015) Breeding signatures of rice improvement revealed by a genomic variation map from a large germplasm collection. *Proc. Natl. Acad. Sci. U. S. A.* **112**, E5411–E5419.

Yamada, S., Kano, A., Tamaoki, D., Miyamoto, A., Shishido, H., Miyoshi, S., Taniguchi, S. *et al*. (2012) Involvement of OsJAZ8 in jasmonate-induced resistance to bacterial blight in rice. *Plant Cell Physiol.* **53**, 2060–2072.

Yang, D.L., Yao, J., Mei, C.S., Tong, X.H., Zeng, L.J., Li, Q., Xiao, L.T. *et al*. (2012) Plant hormone jasmonate prioritizes defense over growth by interfering with gibberellin signaling cascade. *Proc. Natl. Acad. Sci. U. S. A.* **109**, E1192–E1200.

Yang, D.L., Yang, Y. and He, Z. (2013) Roles of plant hormones and their interplay in rice immunity. *Mol. Plant* **6**, 675–685.

Yang, W., Guo, Z., Huang, C., Duan, L., Chen, G., Jiang, N., Fang, W. *et al*. (2014) Combining high-throughput phenotyping and genome-wide association studies to reveal natural genetic variation in rice. *Nat. Commun.* **5**, 5087.

Yang, Z., Hui, S., Lv, Y., Zhang, M., Chen, D., Tian, J., Zhang, H. *et al*. (2022) miR395-regulated sulfate metabolism exploits pathogen sensitivity to sulfate to boost immunity in rice. *Mol. Plant* **15**, 671–688.

Yonemaru, J., Yamamoto, T., Fukuoka, S., Uga, Y., Hori, K. and Yano, M. (2010) Q-TARO: QTL annotation rice online database. *Rice*, **3**, 194–203.

Yuan, M., Chu, Z., Li, X., Xu, C. and Wang, S. (2019) Pathogen-induced expressional loss of function is the key factor in race-specific bacterial resistance conferred by a recessive R gene xa13 in rice. *Plant Cell Physiol*, **50**, 947–955.

Yu, Y., Woo, M.O., Rihua, P. and Koh, H.J. (2020) The *DROOPING LEAF* (*DR*) gene encoding GDSL esterase is involved in silica deposition in rice (*Oryza sativa* L.). *PLoS One*, **15**, e0238887.

Yuan, M., Chu, Z., Li, X., Xu, C. and Wang, S. (2010) The bacterial pathogen *Xanthomonas oryzae* overcomes rice defenses by regulating host copper redistribution. *Plant Cell*, **22**, 3164–3176.

Yuan, M., Ke, Y., Huang, R., Ma, L., Yang, Z., Chu, Z., Xiao, J. *et al*. (2016) A host basal transcription factor is a key component for infection of rice by TALE-carrying bacteria. *Elife*, **5**, e19605.

Zhang, H., Tao, Z., Hong, H., Chen, Z., Wu, C., Li, X., Xiao, J. *et al*. (2016) Transposon-derived small RNA is responsible for modified function of *WRKY45* locus. *Nat. Plants*, **2**, 16016.

Zhang, B., Zhang, L., Li, F., Zhang, D., Liu, X., Wang, H., Xu, Z. *et al*. (2017a) Control of secondary cell wall patterning involves xylan deacetylation by a GDSL esterase. *Nat. Plants*, **3**, 17017.

Zhang, L., Zhang, F., Melotto, M., Yao, J. and He, S.Y. (2017b) Jasmonate signaling and manipulation by pathogens and insects. *J. Exp. Bot.* **68**, 1371–1385.

Zhang, L., Gao, C., Mentink-Vigier, F., Tang, L., Zhang, D., Wang, S., Cao, S. *et al*. (2019) Arabinosyl deacetylase modulates the arabinoxylan acetylation profile and secondary wall formation. *Plant Cell*, **31**, 1113–1126.

Zhang, H., Wang, M., Li, Y., Yan, W., Chang, Z., Ni, H., Chen, Z. *et al*. (2020) GDSL esterase/lipases OsGELP34 and OsGELP110/OsGELP115 are essential for rice pollen development. *J. Integr. Plant Biol.* **62**, 1574–1593.

Zhao, H., Ma, B., Duan, K.X., Li, X.K., Lu, X., Yin, C.C., Tao, J.J. *et al*. (2020a) The GDSL lipase MHZ11 modulates ethylene signaling in rice roots. *Plant Cell*, **32**, 1626–1643.

Zhao, J., Long, T., Wang, Y., Tong, X., Tang, J., Li, J., Wang, H. *et al*. (2020b) *RMS2* encoding a GDSL lipase mediates lipid homeostasis in anthers to determine rice male fertility. *Plant Physiol.* **182**, 2047–2064.

Zhao, Y., Zhu, X., Chen, X. and Zhou, J.M. (2022) From plant immunity to crop disease resistance. *J. Genet. Genomics*, **49**, 693–703.

Supporting information

Additional supporting information may be found online in the Supporting Information section at the end of the article.

Figure S1 *OsGELP77* expression is induced by different pathogens.
Figure S2 Enhanced resistance to *Xoo* of *OsGELP77*-OE plants.
Figure S3 Generation of *OsGELP77* knockout lines.
Figure S4 Alignment of amino acid sequences of functionally characterized plant GDSL proteins.
Figure S5 Contents of individual PC and PE species in the leaves of *OsGELP77*-OE plants and *osgelp77* mutants.
Figure S6 Contents of 28 FFA species in the leaves of *OsGELP77*-OE plants and *osgelp77* mutants.
Figure S7 Contents of 26 DGDG species in the leaves of *OsGELP77*-OE plants and *osgelp77* mutants.
Figure S8 Contents of 37 MGDG species in the leaves of *OsGELP77*-OE plants and *osgelp77* mutants.
Figure S9 Contents of 25 SQDG species in the leaves of *OsGELP77*-OE plants and *osgelp77* mutants.
Figure S10 Contents of 49 DAG species in the leaves of *OsGELP77*-OE plants and *osgelp77* mutants.
Figure S11 Contents of 107 TAG species in the leaves of *OsGELP77*-OE plants and *osgelp77* mutants.
Figure S12 KEGG enrichment analysis of differential lipids between the *osgelp77* mutant and wild type (a) or between the *OsGELP77*-OE plant and wild type (b).
Figure S13 GO enrichment and KEGG pathway analysis of *osgelp77* mutant DEGs.
Figure S14 Modulating *OsGELP77* expression influenced the expression of JA signalling pathway genes.
Figure S15 The *OsGELP77*-OE and *osgelp77* mutant plants showed opposite responses to MeJA treatment in primary shoot and root development.
Figure S16 Relative transcription of *OsGELP77* in the *osmyc2* mutant.
Figure S17 Agronomic traits of *OsGELP77* transgenic lines grown in field.
Figure S18 Colocalization of *OsGELP77* loci with previously reported disease-related QTL derived using different genetic populations.
Figure S19 Expression profiles of *OsGELP77* in different tissues of rice varieties Minghui 63 and Zhenshan 97.
Figure S20 Agronomic traits of NIL-*OsGELP77*^{Hap3} and Zhenshan 97 grown in field.
Table S1 Detailed list of Up-DEGs in the *osgelp77* mutant relative to wild type.
Table S2 Detailed list of Down-DEGs in the *osgelp77* mutant relative to wild type.
Table S3 PCR primers used for vectors construction for *OsGELP77*.
Table S4 PCR primers used for RT-qPCR assay.

